Group V Secreted Phospholipase A_2 Is Upregulated by IL-4 in Human Macrophages and Mediates Phagocytosis via Hydrolysis of Ethanolamine Phospholipids

Julio M. Rubio,*,† Juan P. Rodríguez,*,‡ Luis Gil-de-Gómez,* Carlos Guijas,*,† María A. Balboa,*,† and Jesús Balsinde*,†

Studies on the heterogeneity and plasticity of macrophage populations led to the identification of two major polarization states: classically activated macrophages or M1, induced by IFN-γ plus LPS, and alternatively activated macrophages, induced by IL-4. We studied the expression of multiple phospholipase A_2 enzymes in human macrophages and the effect that polarization of the cells has on their levels. At least 11 phospholipase A_2 genes were found at significant levels in human macrophages, as detected by quantitative PCR. None of these exhibited marked changes after treating the cells with IFN-γ plus LPS. However, macrophage treatment with IL-4 led to strong upregulation of the secreted group V phospholipase A_2 ($sPLA_2$-V), both at the mRNA and protein levels. In parallel with increasing $sPLA_2$-V expression levels, IL-4–treated macrophages exhibited increased phagocytosis of yeast-derived zymosan and bacteria, and we show that both events are causally related, because cells deficient in $sPLA_2$-V exhibited decreased phagocytosis, and cells overexpressing the enzyme manifested higher rates of phagocytosis. Mass spectrometry analyses of lipid changes in the IL-4–treated macrophages suggest that ethanolamine lysophospholipid (LPE) is an $sPLA_2$-V–derived product that may be involved in regulating phagocytosis. Cellular levels of LPE are selectively maintained by $sPLA_2$-V. By supplementing $sPLA_2$-V–deficient cells with LPE, phagocytosis of zymosan or bacteria was fully restored in IL-4–treated cells. Collectively, our results show that $sPLA_2$-V is required for efficient phagocytosis by IL-4–treated human macrophages and provide evidence that $sPLA_2$-V–derived LPE is involved in the process. ***The Journal of Immunology*****, 2015, 194: 3327–3339.**

Phospholipase A_2 (PLA_2) enzymes hydrolyze membrane phospholipids at the *sn-2* position of the glycerol backbone to release a free fatty acid and a lysophospholipid (1). This reaction is especially important when the fatty acid liberated is arachidonic acid (AA), which can be converted into biologically active compounds called eicosanoids (2, 3). Free fatty acids also may act as intracellular signalers on their own (4), and lysophospholipids may initiate signaling through cell surface G protein–coupled receptors (5). The PLA_2 superfamily includes 16 groups of enzymes, and most of these groups contain several subgroups (1). From a functional point of view, PLA_2s can be classified into five major classes: Ca^{2+}-dependent cytosolic enzymes, Ca^{2+}-dependent secreted enzymes, Ca^{2+}-independent cytosolic enzymes, platelet-activating factor acetyl hydrolases, and lysosomal PLA_2s. Of these classes, the first two have repeatedly been implicated in AA mobilization and eicosanoid production in response to stimuli of innate immunity and inflammation. The Ca^{2+}-dependent cytosolic group IVA PLA_2 ($cPLA_2\alpha$) appears to be the critical enzyme in this process and, depending on cell type and stimulus, a secreted Ca^{2+}-dependent PLA_2 may cooperate as well by amplifying the $cPLA_2\alpha$-regulated response (1–3, 6, 7).

Macrophages participate in innate immunity reactions by mediating opsonic (IgG- and complement-mediated) or nonopsonic phagocytosis (via pattern-recognition receptors) of invading microorganisms (8–11). Phagocytosis of foreign material is usually accompanied by the secretion of large amounts of cytokines and AA-derived eicosanoids that, as time passes, contribute to modulate the progress and extent of the inflammatory process. Depending on changes in the microenvironment where the macrophages exert their functions, these cells may exhibit a continuum of activation states, ranging from proinflammatory and antitumor activities to tissue repair and resolution of inflammation. These two poles of the spectrum of states of macrophage activation are termed classic (M1) and alternative (M2) and are thought to play opposing roles during innate immune and inflammatory responses (12–15). Alternative activation of the macrophages induced by Th2 cytokines IL-4 and IL-13 is of particular interest because, in addition to modulating inflammatory repair, it may be implicated in a variety of unforeseen functions, such as glucose homeostasis (16), thermogenesis (17), and learning and memory (18). Alternative macrophage activation is

*Instituto de Biología y Genética Molecular, Consejo Superior de Investigaciones Científicas, Universidad de Valladolid, 47003 Valladolid, Spain; †Centro de Investigación Biomédica en Red de Diabetes y Enfermedades Metabólicas Asociadas, 28029 Madrid, Spain; and ‡Laboratorio de Investigación en Proteínas, Facultad de Ciencias Exactas y Naturales y Agrimensura, Universidad Nacional del Nordeste, 3400 Corrientes, Argentina

Received for publication April 21, 2014. Accepted for publication January 24, 2015.

This work was supported by the Spanish Ministry of Science and Innovation (Grants BFU2010-18826, SAF2010-18831, and SAF2013-48201-R) and the Education Department of the Autonomous Government of Castile and Leon (Grant CSI007U13). L.G.-d.-G. and C.G. were supported by predoctoral fellowships from the Spanish Ministry of Science and Innovation and the University of Valladolid, respectively (Plan de Formación de Personal Investigador Program).

Address correspondence and reprint requests to Prof. J. Balsinde, University of Valladolid School of Medicine, Calle Sanz y Forés 3, 47003 Valladolid, Spain. E-mail address: jbalsinde@ibgm.uva.es

The online version of this article contains supplemental material.

Abbreviations used in this article: AA, arachidonic acid; $cPLA_2\alpha$, Ca^{2+}-dependent cytosolic group IVA PLA_2; LPC, choline lysophospholipid; LPE, ethanolamine lysophospholipid; LPI, lysophosphatidylinositol; PC, choline glycerophospholipid; PE, ethanolamine glycerophospholipid; PI, phosphatidylinositol; PLA_2, phospholipase A_2; qPCR, quantitative PCR; siRNA, small interfering RNA; $sPLA_2$-V, secreted group V PLA_2.

known to enhance the expression of a number of phagocytic receptors, such as MRC-1, and dectin-1, which results in increased endocytosis of mannosylated ligands and other receptor-mediated endocytic processes. These effects are likely intended to ameliorate inflammation via rapid clearance of foreign material and are clearly different from those induced by classic M1 activators, such as IFN-γ with or without LPS (14, 19, 20).

In previous work, we investigated the mechanisms of PLA$_2$-mediated phospholipid turnover in monocytes and macrophages responding to a variety of stimuli of innate immunity and inflammation (21–30). In those studies we took advantage of mass spectrometry–based lipidomic approaches to define, at a molecular species level, the phospholipid substrate specificities of the enzymes involved. In this study, we applied a similar approach to establish changes in the lipidome of human macrophages after polarization/activation to the M1 and M2 states and to relate such changes to the expression of particular PLA$_2$ forms in each of these states. Our goal was to define molecular "fingerprints" of each macrophage state that permit identification of specific traits of the immune response in terms of the lipid metabolic pathways involved. We show that, in human monocyte-derived macrophages, secreted group V PLA$_2$ (sPLA$_2$-V) is strongly upregulated by IL-4 but not by IFN-γ plus LPS. Thus, sPLA$_2$-V constitutes a bona fide marker for human alternatively activated macrophages. We further show that the increased expression of sPLA$_2$-V in IL-4–treated macrophages serves to regulate the cellular levels of ethanolamine lysophospholipids (LPEs) that are necessary to support the elevated phagocytic response that these cells exhibit.

Materials and Methods

Reagents

Ficoll-Paque Plus was purchased from GE Healthcare (Uppsala, Sweden). Gentamicin was from BioWhittaker (Walkersville, MD). The Amaxa Human Macrophage Nucleofector Kit was from Lonza (Basel, Switzerland). Macrophage serum-free medium and RPMI 1640 were from Life Technologies (Carlsbad, CA). Silencer Select small interfering RNAs (siRNAs) to decrease expression of human sPLA$_2$-V mRNA and negative controls were from Ambion (Carlsbad, CA). IFN-γ and IL-4 were from ImmunoTools (Friesoythe, Germany). The plasmid containing human sPLA$_2$-V (31, 32) was generously provided by Dr. Yasuhito Shirai (Kobe University, Kobe, Japan). Zymosan A labeled with Alexa Fluor 594 was from Molecular Probes (Carlsbad, CA). LPE (1-*O*-1′-octadecenyl-*sn*-glycero-3-phosphoethanolamine) was from Avanti (Alabaster, AL). Oligonucleotides were from Eurofins MWG Operon (Hamburg, Germany). The sequences were obtained from PrimerBank (http://pga.mgh.harvard.edu/primerbank/). All other reagents were from Sigma-Aldrich.

Cells

Human monocytes were obtained from pooled buffy coats of healthy male volunteer donors from the Centro de Hemoterapia y Hemodonación de Castilla y León (Valladolid, Spain). Blood cells were diluted 1:1 with PBS, layered over a cushion of Ficoll-Paque, and centrifuged at 750 × *g* for 30 min. The mononuclear cellular layer was recovered and washed three times with PBS, resuspended in RPMI 1640 supplemented with 2 mM L-glutamine and 40 μg/ml gentamicin, and allowed to adhere to plastic in sterile dishes for 2 h at 37˚C. Nonadherent cells were removed by extensively washing with PBS. Pools of cells corresponding to five donors were used in all experiments, and replicates were performed with different pools of cells. Macrophage differentiation (95% monocytes) was achieved by incubating the adhered monocytes in RPMI 1640 supplemented with 2 mM L-glutamine, 40 μg/ml gentamicin, and 5% human serum (which contains M-CSF) in a humidified atmosphere with 5% CO_2, for 2 wk in the absence of exogenous cytokine mixtures, in accordance with previously published procedures (26, 33–36). To generate classically (M1) or alternatively (M2) activated macrophages, the cells were treated with IFN-γ (500 U/ml) plus LPS (10 ng/ml) or IL-4 (1000 U/ml), respectively, in serum-free medium for the indicated periods of time (37, 38). In some experiments, exogenous M-CSF (50 ng/ml) or IL-10 (50 ng/ml) also was used to induce M2 polarization (39). When needed, human macrophages were transfected by the nucleofection technique, following the kit specifications (Amaxa) for human macrophages. Briefly, cells were harvested by treatment with trypsin for 90 min, followed by gentle scraping. After washing, the cells were resuspended in 100 μl human macrophage nucleofector solution. For siRNA experiments, 20 nM sPLA$_2$-V siRNA or control siRNA was added. When the plasmid containing the human sPLA$_2$-V gene was to be transfected, 10 μg plasmid was used, and an empty vector was used as a control. Nucleofection was conducted using the program Y-010, and the cells were resuspended in 400 μl macrophage serum-free medium (Invitrogen) plus 5% heat-inactivated human serum. Cell viability under all experimental conditions used in this study always remained >95%.

Quantitative PCR

Total RNA was extracted from the cells with TRI Reagent solution, according to the manufacturer's instructions, and 2 μg RNA was reverse transcribed using random primers and oligo d(T) and Moloney murine leukemia virus reverse transcriptase (all from Ambion). Quantitative PCR (qPCR) was carried out with an ABI 7500 machine (Applied Biosystems, Carlsbad, CA) using Brilliant III Ultra-Fast SYBR Green qPCR Master Mix (Agilent Technologies, Santa Clara, CA). Cycling conditions were as follows: 1 cycle at 95˚C for 3 min and 40 cycles at 95˚C for 12 s, 60˚C for 15 s, and 72˚C for 28 s. The relative expression of each mRNA was calculated using the algorithm $2^{-\Delta\Delta Ct}$, with cyclophilin A as a control (40).

PLA$_2$ activity assay

Ca^{2+}-dependent PLA$_2$ activity was measured using a modification of the mammalian membrane assay described by Diez et al. (41). Briefly, cell homogenates were incubated for 1–2 h at 37˚C in 100 mM HEPES (pH 7.5) containing 1.3 mM $CaCl_2$ and 100,000 dpm [^{3}H]AA-labeled membrane, used as a substrate, in a final volume of 0.15 ml. Prior to assay, the cell membrane substrate was heated at 57˚C for 5 min to inactivate CoA-independent transacylase activity (42). The assay contained 10 μM bromoenol lactone to completely inhibit endogenous Ca^{2+}-independent PLA$_2$ activity (43) and 1 μM pyrrophenone to completely inhibit cytosolic group IVA PLA$_2$ activity (44). After lipid extraction, free [^{3}H]AA was separated by thin-layer chromatography, using *n*-hexane/ethyl ether/acetic acid (70:30:1) as a mobile phase. These assay conditions were validated previously with regard to time, homogenate protein, and substrate concentration (43–47).

Phagocytosis

For these experiments, opsonized zymosan, labeled with the fluorophore Alexa Fluor 594, or opsonized *Escherichia coli* DH5α bacteria (American Type Culture Collection), transformed with an orange fluorescent protein plasmid (pmOrange; Clontech, Mountain View, CA), was used as a stimulus. The zymosan particles and bacteria were opsonized by incubation with human serum for 20 min at 37˚C, at a ratio of 1 ml serum: 3 mg particles or 9.5 × 10^7 CFU (48). Zymosan was washed three times with PBS and sonicated in RPMI 1640 or HBSS for 15 min.

Macrophages were seeded over glass coverslips, allowed to adhere, washed with RPMI 1640, and resuspended in this medium. Cells were kept at 4˚C for 5 min, and opsonized zymosan (five to seven particles/cell) or opsonized bacteria (10 bacteria/cell) was added. After a 15-min incubation at 37˚C, coverslips were washed with PBS and transferred to plates with RPMI 1640 at 37˚C, and phagocytosis was allowed to proceed for 15–30 min. Reactions were stopped by fixation with 4% paraformaldehyde and 3% sucrose for 15 min; paraformaldehyde was removed by washing the cells three times with PBS. DAPI staining was carried out by treating cells with this dye at a concentration of 1 μg/ml in PBS for 10 min. Coverslips were mounted on microscopy slides with 10 μl a polyvinyl alcohol solution until analysis by fluorescence microscopy. A Leica TCS SP5 X confocal microscope with white laser (470–670 nm) (Leica Microsystem, Wetzlar, Germany) was used for these studies. Images were analyzed with LAS AF v. 2.6.3 (Leica). The phagocytic index was calculated by dividing the number of phagosomes by the total number of cells in a field, which was multiplied by the percentage of phagocytosing cells, as described elsewhere (49, 50).

Immunoblot

The cells were lysed with 20 mM Tris-HCl (pH 7.4) containing 150 mM NaCl, 0.5% Triton X-100, 1 mM Na_3VO_4, 150 mM NaF, 1 mM PMSF, and a protease inhibitor mixture (Sigma) at 4˚C. Homogenates were centrifuged at 12,000 rpm for 10 min. Protein from the supernatants was quantified using a Bradford protein assay kit (Bio-Rad), and 75 μg total protein was separated by standard 15% SDS-PAGE and transferred to polyvinylidene difluoride membranes (Millipore, Bedford, MA) using a Trans-Blot SD semidry transfer system (Bio-Rad) for 20 min and 2.5

mA/cm^2. Membranes were incubated with the corresponding primary Abs. Mouse anti–sPLA$_2$-V IgG (C-4; sc-393606; Santa Cruz Biotechnology, Santa Cruz, CA) was used at 1:100, and mouse anti-β-actin IgG (GE Healthcare) was used at 1:20,000, followed by HRP-conjugated anti-IgG mouse secondary Abs (GE Healthcare). Immunoreactive bands were detected by ECL (Amersham Biosciences, Piscataway, NJ) using Amersham Hyperfilm ECL (GE Healthcare, Amersham, Buckinghamshire, U.K.) and were digitalized with a GS-800 Scanner (Bio-Rad). The resulting digital images were analyzed for quantitative band densitometry at different time exposures within the linear response defined by Quantity One software (version 4.5.2; Bio-Rad).

Liquid chromatography/mass spectrometry analyses of macrophage glycerophospholipids

A cell extract corresponding to 10^7 cells was used for these analyses. The following internal standards were added—600 pmol each 1,2-dipentadecanoyl-*sn*-glycero-3-phosphocholine, 1,2-dilauroyl-*sn*-glycero-3-phosphoethanolamine, and 1,2-dipalmitoyl-*sn*-glycero-3-phosphoinositol—before lipid extraction, according to the method of Bligh and Dyer (51). After evaporation of the organic solvent under vacuum, the lipids were redissolved in 100 μl methanol/water (9:1, v/v) and injected into a high-performance liquid chromatograph equipped with a binary pump Hitachi LaChrom Elite L-2130 and a Hitachi Autosampler L-2200 (Merck). The column was a SUPELCOSIL LC-18 (5-μm particle size, 250 × 2.1 mm) protected by a LC-18 Supelguard (20 × 2.1 mm) Cartridge (both from Sigma-Aldrich). Mobile phase was a gradient of solvent A (methanol/water/*n*-hexane/32% ammonium hydroxide, 87.5:10.5:1.5:0.5, by volume) and solvent B (methanol/*n*-hexane/32% ammonium hydroxide, 87.5:12:0.5, by volume). The gradient was started at 100% solvent A; it was decreased linearly to 65% solvent A, 35% solvent B in 20 min, to 10% solvent A, 90% solvent B in 5 min, and to 0% solvent A, 100% solvent B in an additional 5 min. Flow rate was 0.5 ml/min, and 80 μl lipid extract was injected. The liquid chromatography system was coupled online to a Bruker esquire6000 ion-trap mass spectrometer (Bruker Daltonics, Bremen, Germany). The total flow rate into the column was split, and 0.2 ml/min entered the electrospray interface of the mass spectrometer. Nebulizer gas was set to 30 pounds per square inch, dry gas was set to 8 l/min, and dry temperature was set to 365°C. Ethanolamine glycerophospholipids (PE) and phosphatidylinositol (PI) were detected in negative ion mode with the capillary current set at +3500 V over the initial 25 min as $[M–H]^-$ ions. Choline glycerophospholipid (PC) species were detected over the elution interval from 25 to 35 min in positive ion mode, as $[M+H]^+$ ions, with the capillary current set at −3500 V.

PE and PI molecular species were identified by multiple reaction monitoring experiments on chromatographic effluent by comparison with previously published data (24, 26–30, 52–54). Cutoff parameter was set at m/z 150, and fragmentation amplitude was set at one arbitrary unit. Because of the lability of vinyl ether linkages in acid media, plasmenyl (1-alkyl) and plasmenyl (1-alk′1′-enyl) glycerophospholipids were distinguished by acidifying the samples before lipid extraction. For the identification of acyl chains of PC species, ionization was carried out in negative mode with postcolumn addition of acetic acid at a flow rate of 100 μl/h as $[M+CH_3CO_2]^-$ adducts. Stereospecific assignation of fatty acyl chains was carried out by comparing the relative intensities of the 1-lysophospholipid and 2-lysophospholipid compounds arising in the fragmentation experiments (the signal of the latter predominates over that of the former in ion-trap mass spectrometry) (24, 26–30, 52–54).

Gas chromatography/mass spectrometry analysis of fatty acid methyl esters

After incubations, the cells were washed twice with PBS, and a cell extract corresponding to 10^7 cells was scraped in ice-cold water and sonicated in a tip homogenizer twice for 15 s. Before extraction and separation of lipid classes, internal standards were added. For total phospholipids, 10 nmol 1,2-diheptadecanoyl-*sn*-glycero-3-phosphocholine was added; for triacylglycerol, 10 nmol 1,2,3-triheptadecanoylglycerol was added; and for cholesterol esters, 20 nmol cholesteryl erucate was added. Total lipids were extracted according to Bligh and Dyer (51), and the resulting lipid extract was separated by thin-layer chromatography using *n*-hexane/diethyl ether/acetic acid (70:30:1, by volume) as the mobile phase. Spots corresponding to phospholipids were extracted from the silica with 800 μl methanol, followed by 800 μl chloroform/methanol (1:2, v/v) and 500 μl chloroform/methanol (2:1, v/v). Phospholipids were transmethylated with 500 μl 0.5 M KOH in methanol for 30 min at 37°C, and 500 μl 0.5 M HCl was added to neutralize. Extraction of fatty acid methyl esters was carried out with 1 ml *n*-hexane twice. Analysis of fatty acid methyl esters was carried out in a Agilent 7890A gas chromatograph coupled to an Agilent 5975C mass-selective detector operated in electron impact mode (70 eV) equipped with an Agilent 7693 Autosampler and an Agilent DB23 column (60 m length × 250 μm internal diameter × 0.15 μm film thickness) under the conditions described previously (35, 53). Data analysis was carried out with Agilent G1701EA MSD Productivity Chemstation software, revision E.02.00.

Liquid chromatography/mass spectrometry analyses of eicosanoids

A small amount of butylated hydroxytoluene in methanol (0.01%, w/v) was added to the supernatants to prevent eicosanoid degradation. Deuterated PGE_2 and leukotriene B_4 (200 pmol each) were added as internal standards before extraction. Eicosanoids were extracted using Bond Elut Plexa solid-phase extraction columns (Agilent), following the manufacturer's instructions. Columns were pretreated with 3 ml methanol and 3 ml water. Supernatants were acidified with 0.5% acetic acid, and 10% methanol was added before sample loading. Samples were washed with 3 ml 10% methanol, and lipid products were eluted with 1.5 ml 100% methanol twice. Lipid products were concentrated under vacuum and redissolved in 100 μl solvent A (see below). A total of 90 μl the extract was injected into an Agilent 1260 Infinity high-performance liquid chromatograph equipped with an Agilent G1311C quaternary pump and an Agilent G1329B Autosampler. The column was a SUPELCOSIL LC-18 (250 × 2.1 mm, 5 μm particle size) protected by a LC-18 Supelguard (20 × 2.1 mm) Cartridge (Sigma-Aldrich). The mobile phase consisted of a gradient of solvent A (water/acetonitrile/acetic acid, 70:30:0.02, by volume) and solvent B (acetonitrile/isopropanol, 50:50, by volume). The gradient was started at 100% solvent A, which was decreased linearly to 75% at 3 min, 55% at 11 min, 40% at 13 min, 25% at 18 min, and 10% at 18.5 min. The last solvent mixture was held for an additional 1.5-min period; finally, the column was re-equilibrated with 100% solvent A for 10 min before the next sample injection (30). The flow rate through the column was fixed at 0.6 ml/min, and this flow entered into the electrospray interface of an API2000 triple quadrupole mass spectrometer (Applied Biosystems). The parameters of the source were set as follows: ion spray voltage, −4500 V; curtain gas, 25 pounds per square inch; nebulizer gas, 40 pounds per square inch; desolvation gas, 80 pounds per square inch; and desolvation gas temperature, 525°C. The analyzer mode was set to scheduled multiple-reaction monitoring with negative ionization, defining for each analyte the m/z of the parent ion as Q1 mass and the m/z of its daughter ion fragment (transition) as Q3 mass and associating with the chromatographic retention time to improve the number of analytes collected in a single chromatographic run. The retention time window was set to 120 s. The declustering potential and collision energy for each analyte were optimized by the use of analytical standards. Other parameters were fixed for all analytes: entrance potential, −10 V; focusing potential, −350 V; and collision cell exit potential, −10 V. Quantification was carried out by integrating the chromatographic peaks of each species and comparing with an external calibration curve made with analytical standards (30).

Liquid chromatography/mass spectrometry analyses of lysophospholipids

A cell extract corresponding to 10^7 cells was used for these analyses. The following internal standards were added—200 pmol each 1-tridecanoyl-*sn*-glycero-3-phosphocholine and 1-miristoyl-*sn*-glycero-3-phosphoethanolamine—before lysophospholipid extraction with *n*-butanol. After evaporation of the organic solvent under vacuum, the lipids were redissolved in 100 μl methanol/water (9:1, v/v) and injected into a high-performance liquid chromatograph equipped with a binary pump Hitachi LaChrom Elite L-2130 and a Hitachi Autosampler L-2200 (Merck). The column was a Supelcosil LC-Si (150 × 3 mm, 3 μm particle size) protected by a Supelguard LC-Si guard cartridge (Sigma-Aldrich). Mobile phase was a gradient of solvent A (chloroform/methanol/water/32% ammonium hydroxide, 75:24:5:0.5, by volume) and solvent B (chloroform/methanol/water/32% ammonium hydroxide, 55:39:5.5:0.5, by volume). The gradient was started at 100% solvent A, it was decreased linearly to 50% solvent A in 2 min, it was maintained for 8 min, and finally it was decreased to 0% solvent A in 2 min. Flow rate was 0.5 ml/min, and 50 μl the lipid extract was injected. The liquid chromatography system was coupled online to a Bruker esquire6000 ion-trap mass spectrometer (Bruker Daltonics). The total flow rate into the column was split, and 0.2 ml/min entered into the electrospray interface of the mass spectrometer. Nebulizer gas was set to 30 pounds per square inch, dry gas was set to 8 l/min, and dry temperature was set to 365°C. Ethanolamine and inositol lysophospholipids were detected in negative ion mode with the capillary current set at +3500 V as

$[M–H]^-$ ions. Choline lysophospholipids (LPCs) were detected in positive ion mode as $[M+H]^+$ ions, with the capillary current set at −4000 V. Measurements correspond to the intensity of each species divided by the intensity of the internal standards corresponding to that particular headgroup. No internal standards were available for the lysophosphatidylinositol (LPI) subclass, so the intensity of each species was divided by the total LPI intensity in this case. The amount of internal standard added to each sample was always identical. The relative intensity values were normalized to the measured quantity of protein present in each cell preparation following treatment or not with IL-4 for each condition.

Results

Expression of PLA$_2$ forms in human macrophages

Cells involved in inflammatory reactions are known to express multiple PLA$_2$ forms. Thus, the challenge is to delineate the role that each of these enzymes plays in cell functioning. We began the current study by determining, by qPCR, the expression level of mammalian PLA$_2$s in human monocyte-derived macrophages. All of the PLA$_2$s assessed are listed in Table I. Of these, only the following were expressed at significant levels by the cells (fluorescence signal in reactions with specific primers detected below 30 cycles): PLA$_2$-IID, -IVA, -IVB, -IVC, -V, -VIA, -VIB, -VIC, -VID, -VIE, -VIF, -XIIA, -XV, and -XVI (Supplemental Fig. 1A). In the next series of experiments, we treated the macrophages with LPS/IFN-γ or IL-4 to induce polarization/activation of the macrophages to M1 or M2 phenotypes, respectively, and changes in the expression levels of the various PLA$_2$s were studied. Control measurements indicated that these treatments induced the expected macrophage polarizations to either M1 or M2 phenotypes, as assessed by specific marker analysis (TNF-α, IL-12α, IL-12β, and IL-6 for M1; ARG1, MRC1, and CCL13 for M2) (Fig. 1). Treating the cells with LPS/IFN-γ induced little or no change in the levels of the various PLA$_2$s expressed by the cells (Supplemental Fig. 1B). Unexpectedly, IL-4 induced a strong increase in the expression level of sPLA$_2$-V (150-fold increase at 24 h) (Supplemental Fig. 1B). This is a surprising finding because, in murine macrophages, sPLA$_2$-V was demonstrated to be upregulated by LPS (55–59) and to function primarily to exacerbate inflammatory reactions (60). Immunoblot analyses of sPLA$_2$-V

Table I. Oligonucleotide primers used for detection of PLA$_2$ genes from human macrophage cDNA

PLA$_2$ Group		Primer Sequence (5′–3′)	Amplification Size (bp)	Detection
PLA$_2$-IB	Sense	TGCCAGACACATGACAACTG	97	
	Antisense	ACGAGTATGAATAGGTGTGGGT		
PLA$_2$-IIA	Sense	ATGAAGACCCTCCTACTGTTGG	110	
	Antisense	GCTTCCTTTCCTGTCGTCAACT		
PLA$_2$-IID	Sense	GCAGAGGCCAACCCAAAGA	68	Yes
	Antisense	CAGGTGGTCATAGCAGCAGTCA		
PLA$_2$-IIE	Sense	TGGGCTGTGAGCCCAAA	68	
	Antisense	GCCGGCGCAGAAAATG		
PLA$_2$-IIF	Sense	ACCAGACGTACCGAGAGGAG	122	
	Antisense	CGCTGGGGATTGGTGACTG		
PLA$_2$-III	Sense	AATCAGCACGACTCCATCTCG	132	
	Antisense	GCCGTACATCCTACACCCG		
PLA$_2$-IVA	Sense	ACTCCAGATCCCTATGTGGAAC	194	Yes
	Antisense	GCTGTCCCTAGAGTTTCATCCAT		
PLA$_2$-IVB	Sense	CTGCCAGGTCCTTCTGAGAC	209	Yes
	Antisense	AGACCTGCAGGAGGATGAGA		
PLA$_2$-IVC	Sense	TGAGGACCCCGAAAGGAAAG	146	Yes
	Antisense	GGCTGCTCATTATCTTGTCCC		
PLA$_2$-IVD	Sense	AGCCCCGGATCTGCTTTCT	80	
	Antisense	GGTGAGGTCATACCAGGCATC		
PLA$_2$-IVE	Sense	AGAACGTGCTAGAGTTGAGTGT	109	
	Antisense	TGGGTTTTCTTTCGGAAACAGAG		
PLA$_2$-IVF	Sense	GGCGGGAAACCTACCCATAC	69	
	Antisense	CTGTGCCCCGGATGTTTGT		
PLA$_2$-V	Sense	CAACATTCGCACACAGTCCTA	89	Yes
	Antisense	CACAGAGGTTCACATGGCAG		
PLA$_2$-VIA	Sense	TCACCAACTTGTTCTCTAACCCA	80	Yes
	Antisense	CTCCCGAACTCGGTCACTC		
PLA$_2$-VIB	Sense	CAGCGAGAAAAGATTATCGCAAG	89	Yes
	Antisense	AGCTTTGGGTCAGTTGTTCTTC		
PLA$_2$-VIC	Sense	CTGCAAACTGGAATGGTGCTT	189	Yes
	Antisense	CACCTTCCGCATAATCTTCCG		
PLA$_2$-VID	Sense	GAAGGCCAGGAGTCGGAAC	125	Yes
	Antisense	TGCCTATTTTGCCGGAGATGA		
PLA$_2$-VIE	Sense	GCACCCCTCCTTCAACCTG	132	Yes
	Antisense	ATGACATTCTCGCCGTCTGAC		
PLA$_2$-VIF	Sense	GTGGGATGGAGTCGATTCTTCC	68	Yes
	Antisense	GATGGATACGTGCAGTCGGTT		
PLA$_2$-X	Sense	AACCCCCATCGCCTATATGAA	112	
	Antisense	TCGAGTGTAACAACAGTCGTG		
PLA$_2$-XIIA	Sense	ATCTAAGCCTTTCCCACGTTATG	133	Yes
	Antisense	ATAGCACCTGTCGTGTTGGTT		
PLA$_2$-XIIB	Sense	GCCAACAAATATCGCTGTGATG	54	
	Antisense	GCAGATCGAGTGGAGACACC		
PLA$_2$-XV	Sense	CTGCTGGATTGACAATATCAGGC	250	Yes
	Antisense	CCCGTTTTCATTTGGGGCTC		
PLA$_2$-XVI	Sense	CTGCGAGCACTTTGTGAATGA	150	Yes
	Antisense	TGCTTTTGTCGCTTGTTTCTTG		

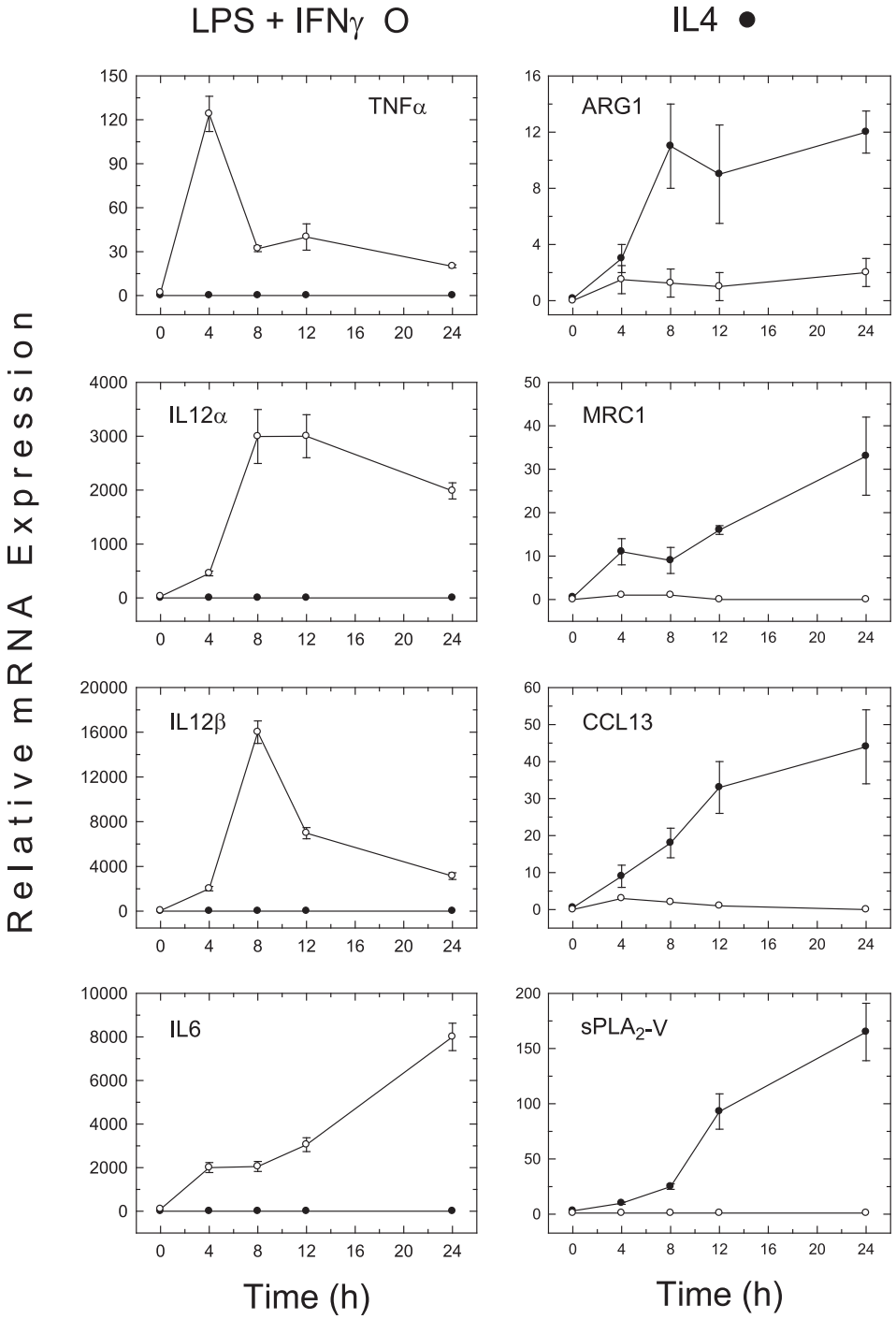

FIGURE 1. Expression of $sPLA_2$-V and representative M1 and M2 genes during human macrophage polarization. The cells were either left untreated (zero time) or treated with 500 U/ml IFN-γ plus 10 ng/ml LPS (○) or 1000 U/ml IL-4 (●) for the indicated times. qPCR for the indicated genes was performed. Data are relative to basal expression levels and normalized to cyclophilin A. Data are average of three independent experiments with triplicate determinations (mean ± SEM).

content in homogenates from IL-4–treated cells indicated a 5–6-fold increase in the expression of the protein at 24 h (Fig. 2A). To assess whether the effect of IL-4 on $sPLA_2$-V was stimulus specific or also was observed with other model stimuli of M2 polarization, we tested the effects of M-CSF and IL-10. The results (Fig. 2B, 2C) indicated that these two stimuli increased $sPLA_2$-V protein expression to levels similar to those found with IL-4, suggesting that elevated expression of $sPLA_2$-V is a general feature of the M2 phenotype.

$sPLA_2$-V regulates phagocytosis in IL-4–treated cells

In agreement with previous observations (13, 14), treating the macrophages with IL-4 increases their capacity to phagocytose yeast-derived zymosan particles. A possible involvement of $sPLA_2$-V in this response was investigated initially by inhibiting expression of the enzyme by siRNA. Using this technology, an ~90% inhibition of $sPLA_2$-V mRNA levels was achieved in IL-4–treated cells, as judged by qPCR (Supplemental Fig. 2A), and in vitro activity assays confirmed a decrease of similar magnitude in total cellular $sPLA_2$ activity, as measured using a natural membrane–based assay (Supplemental Fig. 2B). Importantly, the $sPLA_2$-V–deficient cells exhibited a marked decrease in their ability to phagocytose zymosan particles after IL-4 treatment (Fig. 3A).

To complement the above data, in the next series of experiments we prepared macrophages overexpressing a plasmid containing human $sPLA_2$-V. The cells showed a 15–20-fold increase in mRNA for this enzyme at 24 h, as measured by qPCR

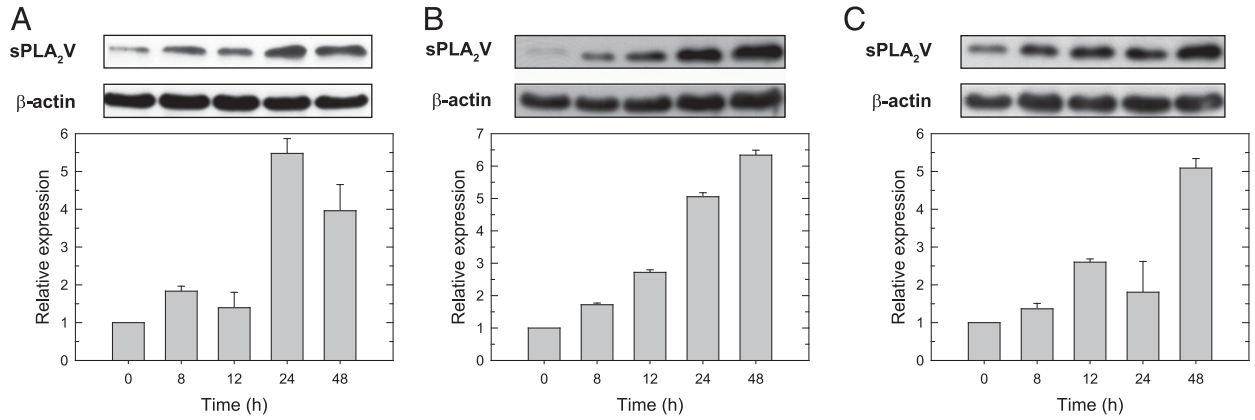

FIGURE 2. Induction of sPLA$_2$-V protein during human macrophage polarization to M2. The cells were either left untreated (zero time) or treated with 1000 U/ml IL-4 (**A**), 50 ng/ml M-CSF (**B**), or 50 ng/ml IL-10 (**C**) for the indicated times. sPLA$_2$-V protein was analyzed by immunoblot (*upper panels*). The blots were quantified from three different experiments (mean ± SEM), and the quantifications are shown (*lower panels*).

(Supplemental Fig. 2A), which translated into a 6–11-fold increase in cellular sPLA$_2$ activity, as measured in a natural membrane-based assay (Supplemental Fig. 2B). Fig. 3B shows that simply overexpressing sPLA$_2$-V into the macrophages was sufficient to produce a significant augmentation of the phagocytic capacity of the cells, which was comparable to that induced by IL-4. Treating sPLA$_2$-V–overexpressing cells with IL-4 did not increase the phagocytic capacity of the cells beyond those levels already attained with either treatment alone (Fig. 3B). The latter finding was not unexpected because the increase in sPLA$_2$-V levels in the overexpressing cells was comparable to that observed in IL-4–treated cells, as judged by activity assay (Supplemental Fig. 2).

To study whether the key role for sPLA$_2$-V in phagocytosis in IL-4–treated cells could be extended to other models of M2 polarization, experiments also were conducted with M-CSF, which, as previously shown in Fig. 2, also increases sPLA$_2$-V to levels comparable to that of IL-4. In keeping with IL-4–treated cells, sPLA$_2$-V–depleted cells treated with M-CSF also showed a significant inhibition of their ability to phagocytose zymosan particles (Supplemental Fig. 3). Collectively, these results highlight a key role for sPLA$_2$-V in regulating phagocytic events in human macrophages polarized to an M2 state.

sPLA$_2$-V–dependent changes in lipid metabolism in IL-4–treated cells

Unlike other sPLA$_2$ family members, such as sPLA$_2$-IIA, most, if not all, biological effects attributed to sPLA$_2$-V are thought to be due to its hydrolytic activity on cell membranes (60–62). Therefore, it was logical to hypothesize that a metabolite produced by sPLA$_2$-V is responsible for its biological effects on IL-4–induced phagocytosis. To identify such a metabolite, we conducted liquid chromatography/mass spectrometry–based lipidomic analyses of major glycerophospholipids to detect changes in the levels of these lipids that may arise as a consequence of cell activation with IL-4 (Fig. 4A–D). Phospholipid species within each class are given in abbreviated form (number of carbon atoms and double bonds of the two lateral chains together) because, in most cases, fragmentation of the m/z peaks yielded fragments corresponding to various species, and it was not possible to unequivocally assign structures to these m/z peaks. A designation of *O-* before the first fatty chain indicates that the *sn*-1 position is ether linked, whereas a P- designation indicates a plasmalogen form (*sn*-1 vinyl ether linkage) (63). In general, no significant alterations were detected in the levels of major phospholipid classes after treating the cells with IL-4 for 24 h, nor was any change detected when sPLA$_2$-V–deficient versus normal cells were used. It should be noted that human macrophages are relatively large cells (diameter > 30 μm) (33, 34); hence, their membrane phospholipid content is quite high (35). Thus, if the hydrolytic action of IL-4–induced sPLA$_2$-V on membrane phospholipids is limited, the small changes involved easily could be obscured by the high phospholipid amount present in the cells. In accord with this, analysis by gas chromatography/mass spectrometry of total phospholipid fatty acids revealed no significant changes in any of the fatty acids measured (Fig. 4E). In some cases, there seemed to be a tendency for the IL-4–treated cells to exhibit mild decreases in certain fatty acids (i.e., 16:0, 18:0 principally, but also 20:4), which were not appreciated when sPLA$_2$-V–deficient cells were used. However, these changes were too small to reach significance.

Liquid chromatography/mass spectrometry analyses of AA-derived eicosanoid metabolites in supernatants revealed that resting human macrophages primarily produced thromboxane B$_2$, PGE$_2$, and 14,15-dihydroxyeicosatrienoic acid, as well as smaller amounts of 15-hydroxyeicosatetraenoic acid, after 24 h in culture (Fig. 5). Production of these eicosanoids was increased modestly by treating the cells with IL-4 (Fig. 5). Use of sPLA$_2$-V–deficient macrophages did not appreciably change the eicosanoid profiles observed in resting or IL-4–treated cells (Fig. 5), suggesting that this limited eicosanoid response likely proceeds without the participation of sPLA$_2$-V.

Lysophospholipids are the other products of PLA$_2$ action on membrane phospholipids. Because of their toxic nature, lysophospholipids accumulate in cells at much lower levels than those of their precursor phospholipids. Given the experiments above, suggesting that the action of IL-4 on phospholipid hydrolysis is, at best, limited, we reasoned that lipid changes probably could be detected in the lysophospholipid fraction because of its lower amount. Using liquid chromatography coupled to mass spectrometry, measurement of lysophospholipid species was carried out, and the effect of depleting the cells of sPLA$_2$-V by siRNA was studied as well. Fig. 6 shows the major lysophospholipid species detected in resting and IL-4–treated human macrophages. IL-4 failed to induce measurable increases in the levels of any of the species analyzed, confirming the limited extent of action of this cytokine on lipid metabolism. However, when sPLA$_2$-V–deficient cells were examined, a very striking change was appreciated: the levels of all LPE species were significantly decreased following exposure to IL-4 (Fig. 6). This decrease was not observed in the otherwise untreated macrophages, implying that it was related to the activation state of the cells. Moreover, the decrease in LPE species was not mirrored by

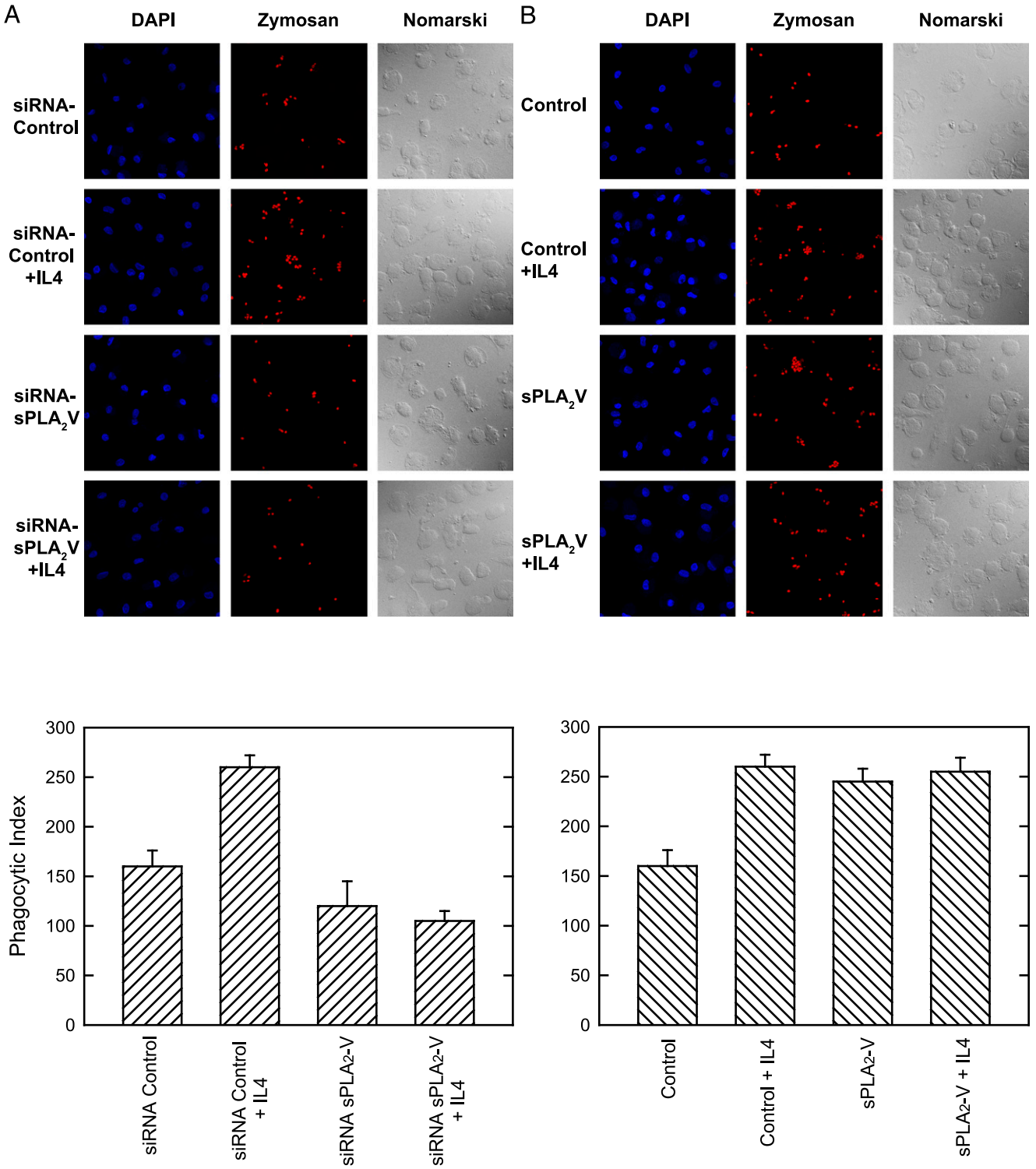

FIGURE 3. $sPLA_2$-V is involved in the phagocytosis of zymosan by IL-4–treated macrophages. Human macrophages, either left untreated or treated with 1000 U/ml IL-4 for 24 h, as indicated, were analyzed for phagocytosis of fluorescent zymosan particles by confocal microscopy (red, *middle columns*). (**A**) Effect of $sPLA_2$-V depletion by siRNA. The cells were treated with siRNA control or siRNA for $sPLA_2$-V, as indicated. (**B**) Effect of sPLA-V overexpression. The cells were transfected with an empty plasmid (control) or a plasmid containing human $sPLA_2$-V, as indicated. DAPI (1 μg/ml) was used to mark the nuclei (blue; *left columns*). Nomarski images are also shown (*right columns*). The average of three independent experiments with triplicate determinations (mean ± SEM) are shown (*bottom panels*). Original magnification ×40.

decreases in any of the other species measured, either of the LPC or LPI class, highlighting a specific effect on a particular class of phospholipids. Because the levels of lysophospholipids in activated cells represent a balance between the opposing actions of activated PLA_2s versus activation of CoA-dependent reacylation and CoA-independent transacylation reactions (2, 3), the significant decrease in LPE in $sPLA_2$-deficient cells constitutes unambiguous evidence that the levels of these particular phospholipid species are maintained by $sPLA_2$-V during IL-4 stimulation of the macrophages. By inference, the data suggest that $sPLA_2$-V–mediated PE hydrolysis leading to LPE formation may constitute an important step in IL-4–induced events in human macrophages.

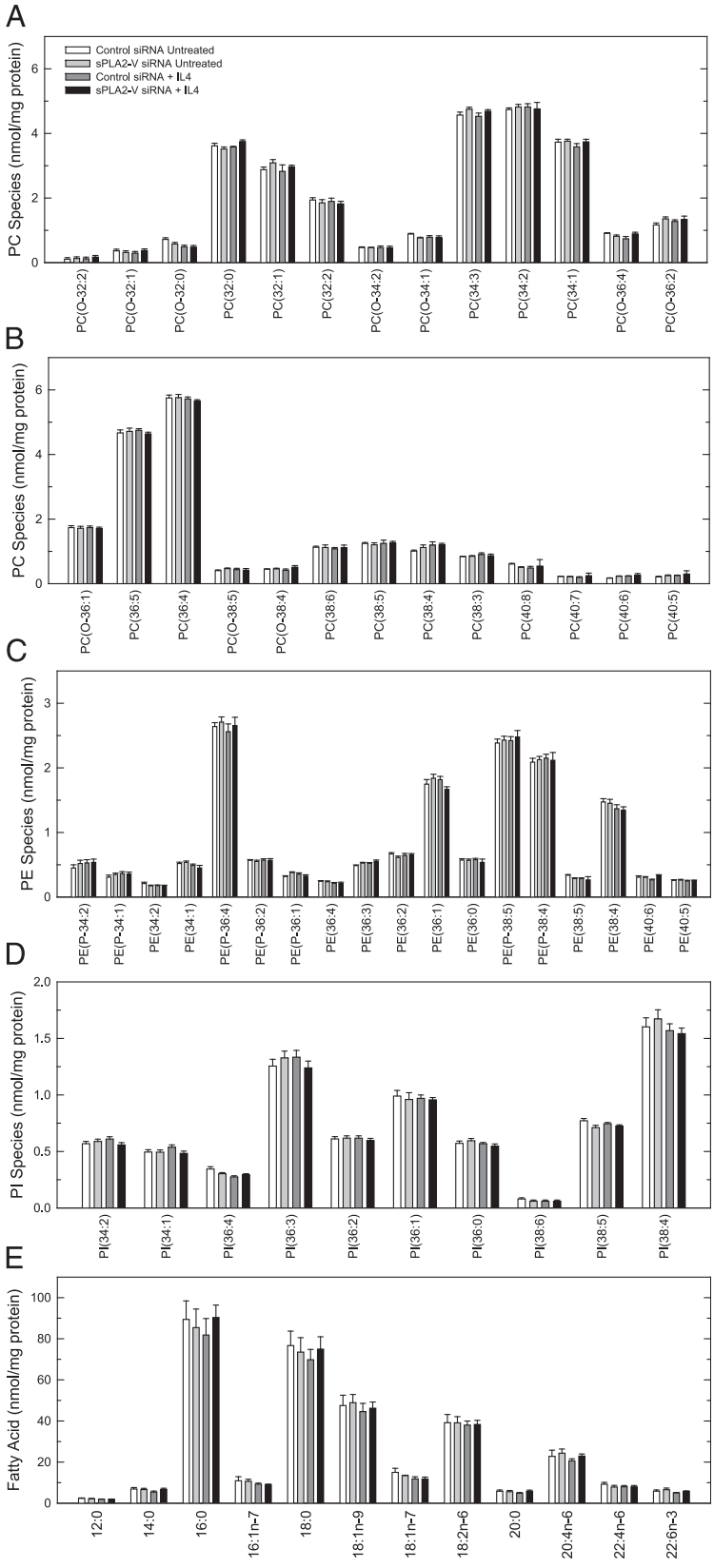

FIGURE 4. Major glycerophospholipid species in human macrophages. Control untreated cells or sPLA$_2$-deficient cells were left untreated or treated with 1000 U/ml IL-4 for 24 h, as indicated. After the incubations, the cellular content of PC (**A** and **B**), PE (**C**), and PI (**D**) molecular species was determined by liquid chromatography/mass spectrometry. (**E**) Total fatty acid in phospholipids was determined by gas chromatography/mass spectrometry. Data are mean ± SEM of three independent experiments with duplicate determinations.

Exogenous LPE restores phagocytosis in sPLA$_2$-V–deficient cells

The above results would be compatible with the possibility that LPE acts as a lipid metabolite that mediates some of the actions of sPLA$_2$-V during stimulation of the cells with IL-4. To examine this possibility, we designed a phagocytosis experiment to assess whether exogenous supplementation of LPE to cells lacking sPLA$_2$-V restores phagocytosis. After the siRNA treatments aimed at blocking sPLA$_2$-V expression, the cells, treated or not with IL-4, were exposed to LPE before phagocytosis was measured; LPC and LPI were used as controls. The lysophospholipids were used at 5 μM, a concentration well below their critical micellular

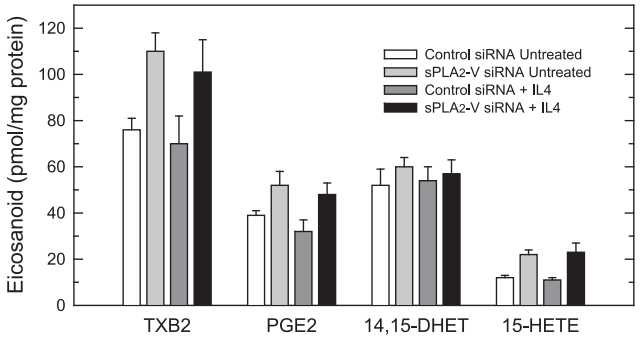

FIGURE 5. Eicosanoids produced by IL-4–treated human macrophages. Control untreated cells or $sPLA_2$-V–deficient cells were either left untreated or treated with 1000 U/ml IL-4 for 24 h, as indicated. After the incubations, the eicosanoid content of supernatants was determined by liquid chromatography/mass spectrometry. Data are mean ± SEM of three independent experiments with duplicate determinations. 14,15-DHET, 14,15-dihydroxyeicosatrienoic acid; 15-HETE, 15-hydroxyeicosatetraenoic acid; TXB2, thromboxane B_2.

concentration, which allows insight into their basic interactions with cell membranes and avoids undesired effects stemming from the formation of vesicles of varying sizes that could interact with the cells in a nonspecific manner (64, 65). The data are shown in Fig. 7. As noted in Fig. 3, the increased phagocytic response of the macrophages to IL-4 was not observed if $sPLA_2$-V–deficient cells were used; however, adding LPE to the sPLA-V–deficient cells fully restored the IL-4 response (Fig. 7). Importantly, LPE did not increase the effect of IL-4 on cells expressing normal $sPLA_2$-V levels, indicating that the signals generated by LPE are already achieved by IL-4, as long as the higher levels of $sPLA_2$-V are preserved. When added in the absence of IL-4, LPE did not exert any effect on its own, as manifested by the finding that phagocytosis of zymosan in control cells was the same as that found in cells treated only with LPE, both under normal and reduced $sPLA_2$-V expression levels. Neither LPC nor LPI, added at the same concentrations as LPE and under the same conditions, exerted any effect, providing support to the specificity of action of LPE (Supplemental Fig. 4). Together, the results shown in Fig. 7 suggest that generation of LPE is a requisite step for IL-4–induced phagocytosis and that this LPE is produced selectively by $sPLA_2$-V.

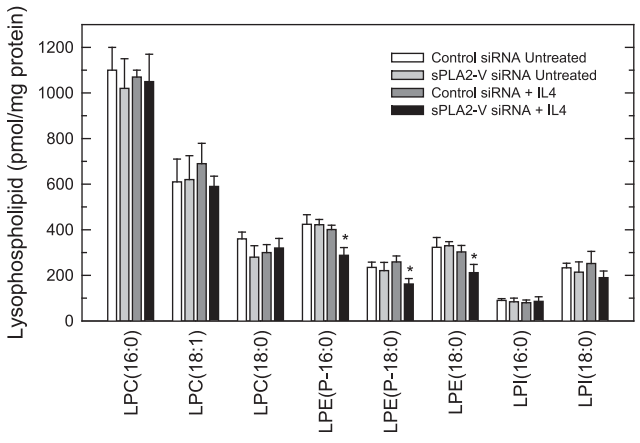

FIGURE 6. Lysophospholipid molecular species of human macrophages. Control untreated cells or $sPLA_2$-V–deficient cells were either left untreated or treated with 1000 U/ml IL-4 for 24 h, as indicated. After the incubations, the cellular content of major 2-lysophospholipids was determined by liquid chromatography/mass spectrometry. Data are mean ± SEM of three independent experiments with duplicate determinations. $^*p < 0.05$.

To make our study more physiologically relevant, we also used a more physiological model of phagocytosis: bacteria. We used *E. coli* expressing orange fluorescent protein, which allowed monitoring of phagocytosis by confocal microscopy. The results (Fig. 8) were wholly comparable to those found for zymosan phagocytosis (Fig. 3); *E. coli* ingestion by IL-4–treated macrophages was markedly diminished by $sPLA_2$-V depletion, and addition of LPE restored the response.

Discussion

Much evidence has been obtained in recent years to support a role for $sPLA_2$-V in regulating innate immune responses. $sPLA_2$-V is present in the secretory granules of WBCs and macrophages, and it is released in response to a large number of innate immune stimuli (60, 61). Part of the enzyme that has been secreted to the extracellular medium may reassociate with the secreting cell and/or be interiorized via several mechanisms to exert its function in an intracellular compartment. Most results on the role of $sPLA_2$-V in pathophysiology have come from studies in mice, and the availability of the $sPLA_2$-V knockout mouse model has provided valuable insights (66, 67). The full eicosanoid response of murine peritoneal macrophages and mast cells to innate immunity stimuli appears to depend on $sPLA_2$-V, which acts to amplify the $cPLA_2\alpha$-initiated response (66–68). In these cells, the enzyme translocates to the phagosome after ingestion of zymosan and regulates phagocytosis by mechanisms that may or may not depend on eicosanoid synthesis, and macrophages from $sPLA_2$-V–null mice exhibit impaired phagocytosis and killing of fungal particles and bacterial clearance (50, 69).

In contrast with the wealth of data in murine cells, little is known about the biological functioning of $sPLA_2$-V in human cells. Studies by Rubin and coworkers (70) demonstrated that the enzyme is secreted by neutrophils and participates in the killing of Gram-negative bacteria, with a limited role in eicosanoid production. Other studies showed that $sPLA_2$-V triggers leukotriene biosynthesis by human neutrophils through activating $cPLA_2\alpha$ (71). However, in human eosinophils, the enzyme was reported to directly hydrolyze phospholipids at the plasma membrane and later at the nuclear envelope in close proximity to eicosanoid biosynthetic enzymes (72). In this study, we sought to determine whether the role of $sPLA_2$-V in innate immunity extends to regulating human macrophage polarization to either M1 or M2 phenotypes. Our data provide evidence that $sPLA_2$-V is important for zymosan phagocytosis by human macrophages and that the regulatory role that the enzyme plays in this process involves generation of LPE, which is produced by the hydrolysis of membrane PE. We found that, in human macrophages, in contrast to murine macrophages, $sPLA_2$-V is not upregulated by cell exposure to the proinflammatory stimuli IFN-γ plus LPS, which polarize the cell to a proinflammatory M1 phenotype. Instead, $sPLA_2$-V is strongly upregulated by IL-4, which polarizes macrophages to an anti-inflammatory M2 state. Although these data could suggest that the biological functioning of $sPLA_2$-V in humans is fundamentally different from that in murine cells, we note that, in both instances, the regulation of phagocytosis by $sPLA_2$-V in human and murine cells might lead to similar outcomes ($sPLA_2$-V regulating phagocytosis in a "positive manner," in that its absence slows phagocytosis). The anti-inflammatory implications of this type of regulation in human cells exposed to IL-4 would be evident, because rapid elimination of foreign material by phagocytosis should accelerate repair mechanisms and the return to homeostasis. A similar purpose could be served as well under classical activation of murine macrophages, because rapid clearance of foreign material would also help to limit the

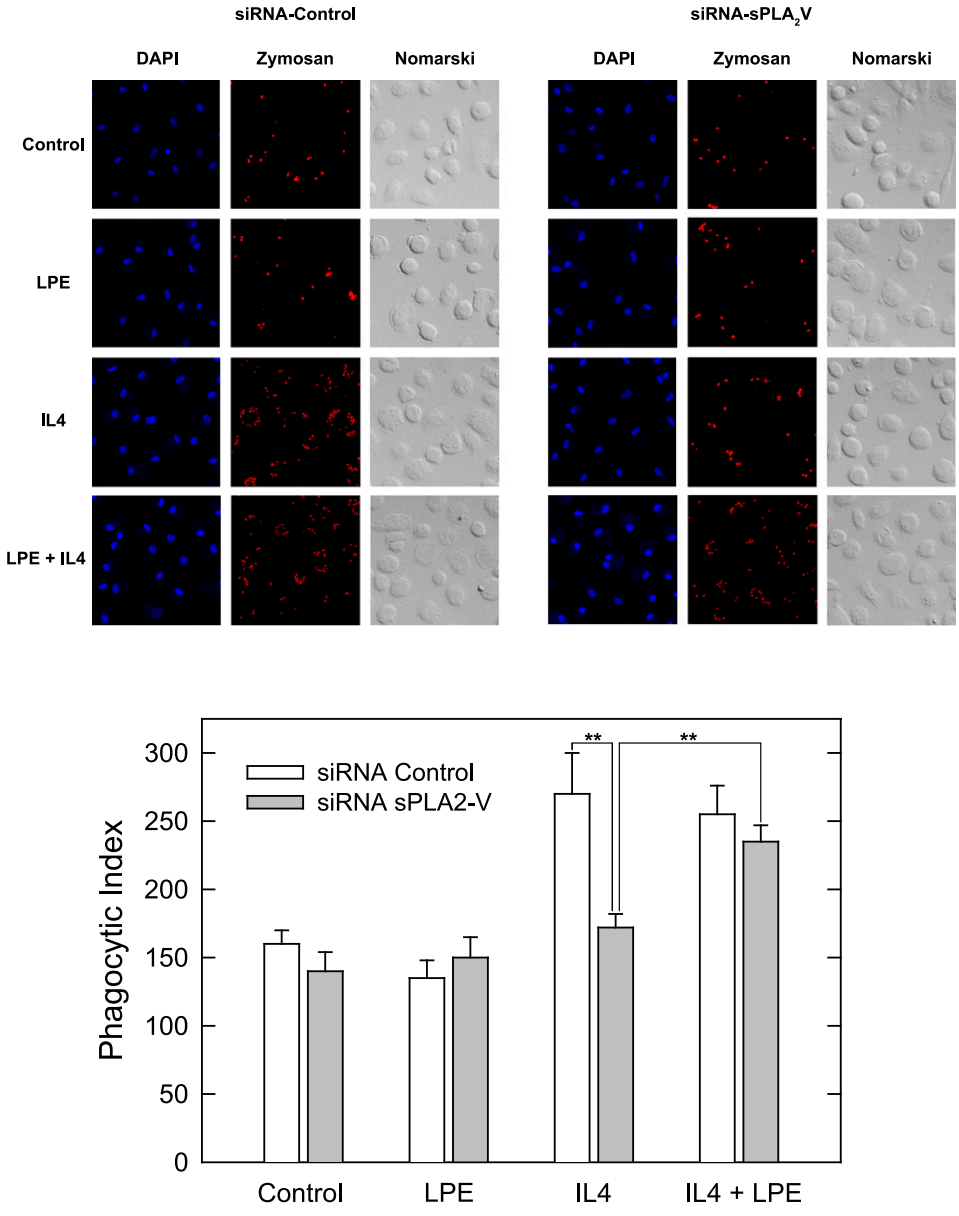

FIGURE 7. LPE restores phagocytosis of zymosan particles in IL-4–treated, sPLA$_2$-V–deficient cells. Human macrophages, either untreated or treated with 1000 U/ml IL-4 for 24 h, as indicated, were analyzed for phagocytosis of fluorescent zymosan particles by confocal microscopy (red color, *middle columns*). The cells were treated with siRNA control or siRNA for sPLA$_2$-V, as indicated. LPE (5 μM) was added, where indicated. DAPI (1 μg/ml) was used to mark the nuclei (blue; *left columns*). Nomarski images are also shown (*right columns*). The average of three independent experiments with triplicate determinations is shown (mean ± SEM) (*bottom panel*). Original magnification ×20. $^{**}p < 0.01$.

deleterious effects of inflammation. Thus, in murine, but not in human, cells, sPLA$_2$-V could function as a bifaceted enzyme, augmenting the early stages of acute inflammation (50, 66) and, in contrast, accelerating the clearance of pathogens (69, 73). A recent report showed that sPLA$_2$-V expression also can be upregulated by IL-4 in murine lung cells (74).

We found no evidence for such a functional plasticity of sPLA$_2$-V in human cells, where the enzyme appears to serve an anti-inflammatory role by regulating the clearance of phagocytosed material. In this regard, it is striking that sPLA$_2$-V translocates to the forming phagosome in zymosan-stimulated murine macrophages (50, 66) but not in zymosan-stimulated human macrophages (33, 34). These data suggest that, at least in humans, the regulatory actions of the enzyme on the phagocytosis process itself occur at a level distinct from that of the phagosome, probably at the plasma membrane level. From that location, the enzyme could promote membrane modifications via phospholipid hydrolysis and the corresponding accumulation of lysophospholipids that allow lateral movement of phagocytic receptors and/or regulatory components. A scenario such as this would be fully consistent with the large body of literature indicating that, after secretion of sPLA$_2$-V to the extracellular medium, the enzyme reassociates with the outer leaflet of the plasma membrane to hydrolyze phospholipids and, in this manner, regulates specific cellular responses (60–62). Thus, sPLA$_2$-V may act in an autocrine or paracrine fashion at different subcellular locations in the cell, depending on cell type and the nature of the activating stimulus.

Formation of LPE in IL-4–treated human macrophages, dependent on sPLA$_2$-V, is the molecular event that we identify in this study as key in the regulation of phagocytosis of both yeast-derived zymosan particles and bacteria, because addition of exogenous LPE fully restores phagocytosis in sPLA$_2$-V–deficient cells. Lysophospholipids have been observed to induce a wide array of effects in a cell-specific manner. Although many of these effects have been attributed to interaction with surface receptors, a number of receptor-independent effects also have been appreciated: partitioning into the lipid bilayer and altering the properties of cell membranes or directly binding to nonreceptor proteins, such as ion channels (65). The latter are of special relevance for LPE because, unlike other lysophospholipids, specific receptors for LPE have not been described (5). Pertinent to the results of this

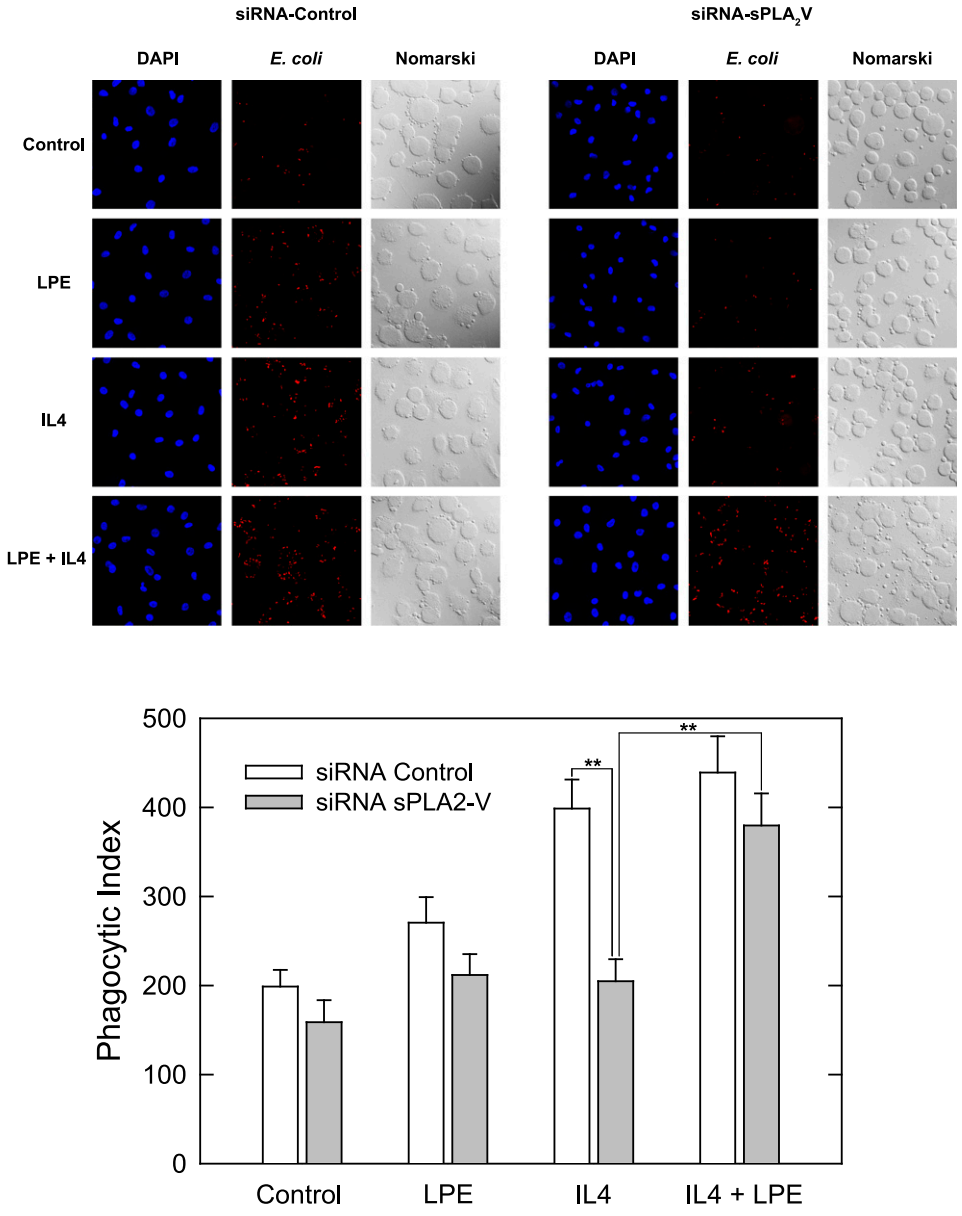

FIGURE 8. LPE restores phagocytosis of bacteria in IL-4–treated, $sPLA_2$-V–deficient cells. Human macrophages, either untreated or treated with 1000 U/ml IL-4 for 24 h, as indicated, were analyzed for phagocytosis of fluorescent bacteria by confocal microscopy (red color, *middle columns*). The cells were treated with siRNA control or siRNA for $sPLA_2$-V, as indicated. LPE (5 μM) was added, where indicated. DAPI (1 μg/ml) was used to mark the nuclei (blue; *left columns*). Nomarski images are also shown (*right columns*). The average of three independent experiments with triplicate determinations is shown (mean ± SEM) (*bottom panel*). Original magnification ×40. $^{**}p < 0.01$.

study, recent studies in neutrophils showed that LPE can induce Ca^{2+}-mediated signaling in neutrophils in a manner that involves participation of the G2A receptor. Importantly, the lysophospholipid effects reported were not due to interaction with the receptor but, rather, occurred via alteration of the structure of the cell membrane (75). In analogy with these results, we speculate that accumulation of LPE, due to increased $sPLA_2$-V activity, may favor oligomerization/interaction of phagocytic receptors at the plasma membrane that enables efficient subsequent signaling. Further, LPE could regulate signaling by altering the structure and fluidity of a variety of microdomains, including lipid rafts. These are specialized microdomains of the plasma that act as docking platforms for receptors and signaling effectors to interact to initiate intracellular responses (76). Interestingly, a variety of receptors that may mediate phagocytosis have been localized to lipid rafts (77–79). Because lipid rafts are enriched in cholesterol and sphingomyelin, as well as in ethanolamine plasmalogens (80, 81), accumulation of LPE at these particular microdomains is a possibility that deserves further consideration. Alternatively, the possibility that loss of function in $sPLA_2$-V–depleted macrophages may, in part, be unrelated to lysophospholipids cannot be ruled out if the enzyme is also exerting noncatalytical functions in the cells. In this regard, recent data showed that $cPLA_2\alpha$ translocation to nascent phagosomes in murine macrophages takes place in a manner that is independent of its enzymatic activity (82).

The process of phagocytosis is accompanied by the rapid generation of AA-derived eicosanoids that promote acute inflammatory responses (83) and may even act to regulate the phagocytic process itself, although the mechanisms involved have not been clearly established. In this regard, $cPLA_2\alpha$, the first rate-limiting enzyme for eicosanoid synthesis, was found to translocate to the phagosome to regulate phagocytosis at various steps, some of which may depend on eicosanoid synthesis, whereas others may not (49, 82). We detected a rather modest production of eicosanoids in IL-4–treated cells that did not change whether $sPLA_2$-V–deficient or normal cells were used. Although $cPLA_2\alpha$ does translocate to the phagosome in human macrophages (33, 34), the lack of involvement of eicosanoids in regulating phagocytosis in human macrophages could constitute another striking difference between human and murine systems, in the light of previous studies showing that alveolar macrophages from 5-lipoxygenase–

null mice have impaired phagocytosis and killing of bacteria (83). However, it should be noted that these effects only were observed for phagocytosis of IgG-opsonized bacteria and not for complement-coated or unopsonized bacteria (83), suggesting that the regulation of phagocytosis by eicosanoids takes place only under specific conditions.

In summary, we provide novel data to indicate that sPLA$_2$-V is required for efficient phagocytosis of zymosan particles and bacteria by IL-4–treated human macrophages and offer evidence that this requirement may involve generation of LPE, likely at the plasma membrane. In addition to its multiple roles in innate immunity and inflammation, sPLA$_2$-V was suggested to participate in the progression of atherosclerosis (84). sPLA$_2$-V–modified low-density lipoproteins promote foam cell formation, and the enzyme has been found in human atherosclerotic lesions. Thus, inhibition of the enzyme is contemplated as a possibly valid therapeutic approach to treating cardiovascular disease. Although recent trials testing the effect of varespladib, an inhibitor of the closely related enzyme sPLA$_2$-IIA that also can block, at least in part, sPLA$_2$-V, provided discouraging results (85, 86), our results implicating sPLA$_2$-V in regulating phagocytosis in human macrophages suggest that possible cardiovascular benefits of inhibiting sPLA$_2$-V could compromise innate immune responses to microorganism infection and, hence, delay resolution of inflammation.

Acknowledgments

We thank Montse Duque and Yolanda Noriega for expert technical help. Centro de Investigación Biomédica en Red de Diabetes y Enfermedades Metabólicas Asociadas is an initiative of Instituto de Salud Carlos III.

Disclosures

The authors have no financial conflicts of interest.

References

1. Dennis, E. A., J. Cao, Y. H. Hsu, V. Magrioti, and G. Kokotos. 2011. Phospholipase A$_2$ enzymes: physical structure, biological function, disease implication, chemical inhibition, and therapeutic intervention. *Chem. Rev.* 111: 6130–6185.
2. Pérez-Chacón, G., A. M. Astudillo, D. Balgoma, M. A. Balboa, and J. Balsinde. 2009. Control of free arachidonic acid levels by phospholipases A$_2$ and lysophospholipid acyltransferases. *Biochim. Biophys. Acta* 1791: 1103–1113.
3. Astudillo, A. M., D. Balgoma, M. A. Balboa, and J. Balsinde. 2012. Dynamics of arachidonic acid mobilization by inflammatory cells. *Biochim. Biophys. Acta* 1821: 249–256.
4. Brash, A. R. 2001. Arachidonic acid as a bioactive molecule. *J. Clin. Invest.* 107: 1339–1345.
5. Kihara, Y., M. Maceyka, S. Spiegel, and J. Chun. 2014. Lysophospholipid receptor nomenclature review: IUPHAR Review 8. *Br. J. Pharmacol.* 171: 3575–3594.
6. Balsinde, J., M. V. Winstead, and E. A. Dennis. 2002. Phospholipase A(2) regulation of arachidonic acid mobilization. *FEBS Lett.* 531: 2–6.
7. Leslie, C. C. 2004. Regulation of arachidonic acid availability for eicosanoid production. *Biochem. Cell Biol.* 82: 1–17.
8. Gordon, S. 2002. Pattern recognition receptors: doubling up for the innate immune response. *Cell* 111: 927–930.
9. Taylor, P. R., S. V. Tsoni, J. A. Willment, K. M. Dennehy, M. Rosas, H. Findon, K. Haynes, C. Steele, M. Botto, S. Gordon, and G. D. Brown. 2007. Dectin-1 is required for beta-glucan recognition and control of fungal infection. *Nat. Immunol.* 8: 31–38.
10. Elsori, D. H., V. P. Yakubenko, T. Roome, P. S. Thiagarajan, A. Bhattacharjee, S. P. Yadav, and M. K. Cathcart. 2011. Protein kinase Cδ is a critical component of Dectin-1 signaling in primary human monocytes. *J. Leukoc. Biol.* 90: 599–611.
11. Underhill, D. M. 2003. Macrophage recognition of zymosan particles. *J. Endotoxin Res.* 9: 176–180.
12. Vega, M. A., and A. L. Corbí. 2006. Human macrophage activation: too many functions and phenotypes for a single cell type. *Inmunología* 25: 248–272.
13. Mosser, D. M., and J. P. Edwards. 2008. Exploring the full spectrum of macrophage activation. *Nat. Rev. Immunol.* 8: 958–969.
14. Gordon, S., and F. O. Martínez. 2010. Alternative activation of macrophages: mechanism and functions. *Immunity* 32: 593–604.
15. Sica, A., and A. Mantovani. 2012. Macrophage plasticity and polarization: in vivo veritas. *J. Clin. Invest.* 122: 787–795.
16. Wu, D., A. B. Molofsky, H. E. Liang, R. R. Ricardo-Gonzalez, H. A. Jouihan, J. K. Bando, A. Chawla, and R. M. Locksley. 2011. Eosinophils sustain adipose alternatively activated macrophages associated with glucose homeostasis. *Science* 332: 243–247.
17. Nguyen, K. D., Y. Qiu, X. Cui, Y. P. Goh, J. Mwangi, T. David, L. Mukundan, F. Brombacher, R. M. Locksley, and A. Chawla. 2011. Alternatively activated macrophages produce catecholamines to sustain adaptive thermogenesis. *Nature* 480: 104–108.
18. Derecki, N. C., A. N. Cardani, C. H. Yang, K. M. Quinnies, A. Crihfield, K. R. Lynch, and J. Kipnis. 2010. Regulation of learning and memory by meningeal immunity: a key role for IL-4. *J. Exp. Med.* 207: 1067–1080.
19. Gordon, S. 2003. Alternative activation of macrophages. *Nat. Rev. Immunol.* 3: 23–35.
20. Martinez, F. O., L. Helming, and S. Gordon. 2009. Alternative activation of macrophages: an immunologic functional perspective. *Annu. Rev. Immunol.* 27: 451–483.
21. Ruipérez, V., J. Casas, M. A. Balboa, and J. Balsinde. 2007. Group V phospholipase A$_2$-derived lysophosphatidylcholine mediates cyclooxygenase-2 induction in lipopolysaccharide-stimulated macrophages. *J. Immunol.* 179: 631–638.
22. Pindado, J., J. Balsinde, and M. A. Balboa. 2007. TLR3-dependent induction of nitric oxide synthase in RAW 264.7 macrophage-like cells via a cytosolic phospholipase A2/cyclooxygenase-2 pathway. *J. Immunol.* 179: 4821–4828.
23. Ruipérez, V., A. M. Astudillo, M. A. Balboa, and J. Balsinde. 2009. Coordinate regulation of TLR-mediated arachidonic acid mobilization in macrophages by group IVA and group V phospholipase A$_2$s. *J. Immunol.* 182: 3877–3883.
24. Balgoma, D., A. M. Astudillo, G. Pérez-Chacón, O. Montero, M. A. Balboa, and J. Balsinde. 2010. Markers of monocyte activation revealed by lipidomic profiling of arachidonic acid-containing phospholipids. *J. Immunol.* 184: 3857–3865.
25. Pérez-Chacón, G., A. M. Astudillo, V. Ruipérez, M. A. Balboa, and J. Balsinde. 2010. Signaling role for lysophosphatidylcholine acyltransferase 3 in receptor-regulated arachidonic acid reacylation reactions in human monocytes. *J. Immunol.* 184: 1071–1078.
26. Valdearcos, M., E. Esquinas, C. Meana, L. Gil-de-Gómez, C. Guijas, J. Balsinde, and M. A. Balboa. 2011. Subcellular localization and role of lipin-1 in human macrophages. *J. Immunol.* 186: 6004–6013.
27. Astudillo, A. M., G. Pérez-Chacón, C. Meana, D. Balgoma, A. Pol, M. A. Del Pozo, M. A. Balboa, and J. Balsinde. 2011. Altered arachidonate distribution in macrophages from caveolin-1 null mice leading to reduced eicosanoid synthesis. *J. Biol. Chem.* 286: 35299–35307.
28. Guijas, C., A. M. Astudillo, L. Gil-de-Gómez, J. M. Rubio, M. A. Balboa, and J. Balsinde. 2012. Phospholipid sources for adrenic acid mobilization in RAW 264.7 macrophages. Comparison with arachidonic acid. *Biochim. Biophys. Acta* 1821: 1386–1393.
29. Gil-de-Gómez, L., A. M. Astudillo, C. Meana, J. M. Rubio, C. Guijas, M. A. Balboa, and J. Balsinde. 2013. A phosphatidylinositol species acutely generated by activated macrophages regulates innate immune responses. *J. Immunol.* 190: 5169–5177.
30. Gil-de-Gómez, L., A. M. Astudillo, C. Guijas, V. Magrioti, G. Kokotos, M. A. Balboa, and J. Balsinde. 2014. Cytosolic group IVA and calcium-independent group VIA phospholipase A$_2$s act on distinct phospholipid pools in zymosan-stimulated mouse peritoneal macrophages. *J. Immunol.* 192: 752–762.
31. Balboa, M. A., Y. Shirai, G. Gaietta, M. H. Ellisman, J. Balsinde, and E. A. Dennis. 2003. Localization of group V phospholipase A$_2$ in caveolin-enriched granules in activated P388D$_1$ macrophage-like cells. *J. Biol. Chem.* 278: 48059–48065.
32. Shirai, Y., J. Balsinde, and E. A. Dennis. 2005. Localization and functional interrelationships among cytosolic Group IV, secreted Group V, and Ca^{2+}-independent Group VI phospholipase A$_2$s in P388D$_1$ macrophages using GFP/RFP constructs. *Biochim. Biophys. Acta* 1735: 119–129.
33. Casas, J., C. Meana, E. Esquinas, M. Valdearcos, J. Pindado, J. Balsinde, and M. A. Balboa. 2009. Requirement of JNK-mediated phosphorylation for translocation of group IVA phospholipase A$_2$ to phagosomes in human macrophages. *J. Immunol.* 183: 2767–2774.
34. Casas, J., M. Valdearcos, J. Pindado, J. Balsinde, and M. A. Balboa. 2010. The cationic cluster of group IVA phospholipase A$_2$ (Lys488/Lys541/Lys543/Lys544) is involved in translocation of the enzyme to phagosomes in human macrophages. *J. Lipid Res.* 51: 388–399.
35. Guijas, C., G. Pérez-Chacón, A. M. Astudillo, J. M. Rubio, L. Gil-de-Gómez, M. A. Balboa, and J. Balsinde. 2012. Simultaneous activation of p38 and JNK by arachidonic acid stimulates the cytosolic phospholipase A$_2$-dependent synthesis of lipid droplets in human monocytes. *J. Lipid Res.* 53: 2343–2354.
36. Valdearcos, M., E. Esquinas, C. Meana, L. Peña, L. Gil-de-Gómez, J. Balsinde, and M. A. Balboa. 2012. Lipin-2 reduces proinflammatory signaling induced by saturated fatty acids in macrophages. *J. Biol. Chem.* 287: 10894–10904.
37. Mantovani, A., A. Sica, S. Sozzani, P. Allavena, A. Vecchi, and M. Locati. 2004. The chemokine system in diverse forms of macrophage activation and polarization. *Trends Immunol.* 25: 677–686.
38. Martínez, F. O., and S. Gordon. 2014. The M1 and M2 paradigm of macrophage activation: time for reassessment. *F1000Prime Rep.* 6: 13.
39. Martínez, F. O., L. Helming, R. Milde, A. Varin, B. N. Melgert, C. Draijer, B. Thomas, M. Fabbri, A. Crawshaw, L. P. Ho, et al. 2013. Genetic programs expressed in resting and IL-4 alternatively activated mouse and human macrophages: similarities and differences. *Blood* 121: e57–e69.
40. Livak, K. J., and T. D. Schmittgen. 2001. Analysis of relative gene expression data using real-time quantitative PCR and the 2(−Delta Delta C(T)) Method. *Methods* 25: 402–408.

41. Diez, E., J. Balsinde, M. Aracil, and A. Schüller. 1987. Ethanol induces release of arachidonic acid but not synthesis of eicosanoids in mouse peritoneal macrophages. *Biochim. Biophys. Acta* 921: 82–89.
42. Winkler, J. D., C. M. Sung, C. F. Bennett, and F. H. Chilton. 1991. Characterization of CoA-independent transacylase activity in U937 cells. *Biochim. Biophys. Acta* 1081: 339–346.
43. Balsinde, J. 2002. Roles of various phospholipases A_2 in providing lysophospholipid acceptors for fatty acid phospholipid incorporation and remodelling. *Biochem. J.* 364: 695–702.
44. Balboa, M. A., and J. Balsinde. 2002. Involvement of calcium-independent phospholipase A_2 in hydrogen peroxide-induced accumulation of free fatty acids in human U937 cells. *J. Biol. Chem.* 277: 40384–40389.
45. Pérez, R., R. Melero, M. A. Balboa, and J. Balsinde. 2004. Role of group VIA calcium-independent phospholipase A_2 in arachidonic acid release, phospholipid fatty acid incorporation, and apoptosis in U937 cells responding to hydrogen peroxide. *J. Biol. Chem.* 279: 40385–40391.
46. Pérez, R., M. A. Balboa, and J. Balsinde. 2006. Involvement of group VIA calcium-independent phospholipase A_2 in macrophage engulfment of hydrogen peroxide-treated U937 cells. *J. Immunol.* 176: 2555–2561.
47. Balboa, M. A., R. Pérez, and J. Balsinde. 2008. Calcium-independent phospholipase A_2 mediates proliferation of human promonocytic U937 cells. *FEBS J.* 275: 1915–1924.
48. Brouwer, N., K. M. Dolman, M. van Houdt, M. Sta, D. Roos, and T. W. Kuijpers. 2008. Mannose-binding lectin (MBL) facilitates opsonophagocytosis of yeasts but not of bacteria despite MBL binding. *J. Immunol.* 180: 4124–4132.
49. Girotti, M., J. H. Evans, D. Burke, and C. C. Leslie. 2004. Cytosolic phospholipase A_2 translocates to forming phagosomes during phagocytosis of zymosan in macrophages. *J. Biol. Chem.* 279: 19113–19121.
50. Balestrieri, B., V. W. Hsu, H. Gilbert, C. C. Leslie, W. K. Han, J. V. Bonventre, and J. P. Arm. 2006. Group V secretory phospholipase A_2 translocates to the phagosome after zymosan stimulation of mouse peritoneal macrophages and regulates phagocytosis. *J. Biol. Chem.* 281: 6691–6698.
51. Bligh, E. G., and W. J. Dyer. 1959. A rapid method of total lipid extraction and purification. *Can. J. Biochem. Physiol.* 37: 911–917.
52. Balgoma, D., O. Montero, M. A. Balboa, and J. Balsinde. 2008. Calcium-independent phospholipase A_2-mediated formation of 1,2-diarachidonoylglycerophosphoinositol in monocytes. *FEBS J.* 275: 6180–6191.
53. Astudillo, A. M., G. Pérez-Chacón, D. Balgoma, L. Gil-de-Gómez, V. Ruipérez, C. Guijas, M. A. Balboa, and J. Balsinde. 2011. Influence of cellular arachidonic acid levels on phospholipid remodeling and CoA-independent transacylase activity in human monocytes and U937 cells. *Biochim. Biophys. Acta* 1811: 97–103.
54. Dumlao, D. S., M. W. Buczynski, P. C. Norris, R. Harkewicz, and E. A. Dennis. 2011. High-throughput lipidomic analysis of fatty acid derived eicosanoids and N-acylethanolamines. *Biochim. Biophys. Acta* 1811: 724–736.
55. Shinohara, H., M. A. Balboa, C. A. Johnson, J. Balsinde, and E. A. Dennis. 1999. Regulation of delayed prostaglandin production in activated $P388D_1$ macrophages by group IV cytosolic and group V secretory phospholipase A_2s. *J. Biol. Chem.* 274: 12263–12268.
56. Balsinde, J., H. Shinohara, L. J. Lefkowitz, C. A. Johnson, M. A. Balboa, and E. A. Dennis. 1999. Group V phospholipase $A_{(2)}$-dependent induction of cyclooxygenase-2 in macrophages. *J. Biol. Chem.* 274: 25967–25970.
57. Balsinde, J., M. A. Balboa, S. Yedgar, and E. A. Dennis. 2000. Group V phospholipase $A_{(2)}$-mediated oleic acid mobilization in lipopolysaccharide-stimulated $P388D_{(1)}$ macrophages. *J. Biol. Chem.* 275: 4783–4786.
58. Balsinde, J., M. A. Balboa, and E. A. Dennis. 2000. Identification of a third pathway for arachidonic acid mobilization and prostaglandin production in activated $P388D_1$ macrophage-like cells. *J. Biol. Chem.* 275: 22544–22549.
59. Sawada, H., M. Murakami, A. Enomoto, S. Shimbara, and I. Kudo. 1999. Regulation of type V phospholipase A_2 expression and function by proinflammatory stimuli. *Eur. J. Biochem.* 263: 826–835.
60. Balestrieri, B., and J. P. Arm. 2006. Group V $sPLA_2$: classical and novel functions. *Biochim. Biophys. Acta* 1761: 1280–1288.
61. Cho, W. 2000. Structure, function, and regulation of group V phospholipase $A_{(2)}$. *Biochim. Biophys. Acta* 1488: 48–58.
62. Murakami, M., Y. Taketomi, C. Girard, K. Yamamoto, and G. Lambeau. 2010. Emerging roles of secreted phospholipase A_2 enzymes: Lessons from transgenic and knockout mice. *Biochimie* 92: 561–582.
63. Fahy, E., S. Subramaniam, H. A. Brown, C. K. Glass, A. H. Merrill, Jr., R. C. Murphy, C. R. Raetz, D. W. Russell, Y. Seyama, W. Shaw, et al. 2005. A comprehensive classification system for lipids. *J. Lipid Res.* 46: 839–861.
64. Stafford, R. E., T. Fanni, and E. A. Dennis. 1989. Interfacial properties and critical micelle concentration of lysophospholipids. *Biochemistry* 28: 5113–5120.
65. Grzelczyk, A., and E. Gendaszewska-Darmach. 2013. Novel bioactive glycerol-based lysophospholipids: new data — new insight into their function. *Biochimie* 95: 667–679.
66. Satake, Y., B. L. Diaz, B. Balestrieri, B. K. Lam, Y. Kanaoka, M. J. Grusby, and J. P. Arm. 2004. Role of group V phospholipase A_2 in zymosan-induced eicosanoid generation and vascular permeability revealed by targeted gene disruption. *J. Biol. Chem.* 279: 16488–16494.
67. Diaz, B. L., Y. Satake, E. Kikawada, B. Balestrieri, and J. P. Arm. 2006. Group V secretory phospholipase A_2 amplifies the induction of cyclooxygenase 2 and delayed prostaglandin D_2 generation in mouse bone marrow culture-derived mast cells in a strain-dependent manner. *Biochim. Biophys. Acta* 1761: 1489–1497.
68. Kikawada, E., J. V. Bonventre, and J. P. Arm. 2007. Group V secretory PLA_2 regulates TLR2-dependent eicosanoid generation in mouse mast cells through amplification of ERK and $cPLA_2\alpha$ activation. *Blood* 110: 561–567.
69. Balestrieri, B., A. Maekawa, W. Xing, M. H. Gelb, H. R. Katz, and J. P. Arm. 2009. Group V secretory phospholipase A_2 modulates phagosome maturation and regulates the innate immune response against *Candida albicans*. *J. Immunol.* 182: 4891–4898.
70. Degousee, N., F. Ghomashchi, E. Stefanski, A. Singer, B. P. Smart, N. Borregaard, R. Reithmeier, T. F. Lindsay, C. Lichtenberger, W. Reinisch, et al. 2002. Groups IV, V, and X phospholipases A2s in human neutrophils: role in eicosanoid production and gram-negative bacterial phospholipid hydrolysis. *J. Biol. Chem.* 277: 5061–5073.
71. Kim, K. P., J. D. Rafter, L. Bittova, S. K. Han, Y. Snitko, N. M. Muñoz, A. R. Leff, and W. Cho. 2001. Mechanism of human group V phospholipase A_2 (PLA_2)-induced leukotriene biosynthesis in human neutrophils. A potential role of heparan sulfate binding in PLA_2 internalization and degradation. *J. Biol. Chem.* 276: 11126–11134.
72. Muñoz, N. M., Y. J. Kim, A. Y. Meliton, K. P. Kim, S. K. Han, E. Boetticher, E. O'Leary, S. Myou, X. Zhu, J. V. Bonventre, et al. 2003. Human group V phospholipase A_2 induces group IVA phospholipase A_2-independent cysteinyl leukotriene synthesis in human eosinophils. *J. Biol. Chem.* 278: 38813–38820.
73. Boilard, E., Y. Lai, K. Larabee, B. Balestrieri, F. Ghomashchi, D. Fujioka, R. Gobezie, J. S. Coblyn, M. E. Weinblatt, E. M. Massarotti, et al. 2010. A novel anti-inflammatory role for secretory phospholipase A_2 in immune complex-mediated arthritis. *EMBO Mol. Med.* 2: 172–187.
74. Ohta, S., M. Imamura, W. Xing, J. A. Boyce, and B. Balestrieri. 2013. Group V secretory phospholipase A_2 is involved in macrophage activation and is sufficient for macrophage effector functions in allergic pulmonary inflammation. *J. Immunol.* 190: 5927–5938.
75. Frasch, S. C., K. Zemski-Berry, R. C. Murphy, N. Borregaard, P. M. Henson, and D. L. Bratton. 2007. Lysophospholipids of different classes mobilize neutrophil secretory vesicles and induce redundant signaling through G2A. *J. Immunol.* 178: 6540–6548.
76. Simons, K., and J. L. Sampaio. 2011. Membrane organization and lipid rafts. *Cold Spring Harb. Perspect. Biol.* 3: a004697.
77. García-García, E., E. J. Brown, and C. Rosales. 2007. Transmembrane mutations to FcgammaRIIA alter its association with lipid rafts: implications for receptor signaling. *J. Immunol.* 178: 3048–3058.
78. Beekman, J. M., J. A. van der Linden, J. G. van de Winkel, and J. H. Leusen. 2008. FcgammaRI (CD64) resides constitutively in lipid rafts. *Immunol. Lett.* 116: 149–155.
79. Bournazos, S., S. P. Hart, L. H. Chamberlain, M. J. Glennie, and I. Dransfield. 2009. Association of FcgammaRIIa (CD32a) with lipid rafts regulates ligand binding activity. *J. Immunol.* 182: 8026–8036.
80. Pike, L. J., X. Han, K.-N. Chung, and R. Gross. 2002. Lipid rafts are enriched in arachidonic acid and plasmenylethanolamine and their composition is independent of caveolin-1 expression: a quantitative electrospray ionization/mass spectrometric analysis. *Biochemistry* 41: 2075–2088.
81. Gorgas, K., A. Teigler, D. Komljenovic, and W. W. Just. 2006. The ether lipid-deficient mouse: tracking down plasmalogen functions. *Biochim. Biophys. Acta* 1763: 1511–1526.
82. Zizza, P., C. Iurisci, M. Bonazzi, P. Cossart, C. C. Leslie, D. Corda, and S. Mariggiò. 2012. Phospholipase $A_2IV\alpha$ regulates phagocytosis independent of its enzymatic activity. *J. Biol. Chem.* 287: 16849–16859.
83. Peters-Golden, M., C. Canetti, P. Mancuso, and M. J. Coffey. 2005. Leukotrienes: underappreciated mediators of innate immune responses. *J. Immunol.* 174: 589–594.
84. Guijas, C., J. P. Rodríguez, J. M. Rubio, M. A. Balboa, and J. Balsinde. 2014. Phospholipase A_2 regulation of lipid droplet formation. *Biochim. Biophys. Acta* 1841: 1661–1671.
85. Stoekenbroek, R. M., J. J. P. Kastelein, and G. K. Hovingh. 2013. Recent failures in antiatherosclerotic drug development: examples from the thyroxin receptor agonist, the secretory phospholipase A_2 antagonist, and the acyl coenzyme A: cholesterol acyltransferase inhibitor programs. *Curr. Opin. Lipidol.* 24: 459–466.
86. Nicholls, S. J., J. J. Kastelein, G. G. Schwartz, D. Bash, R. S. Rosenson, M. A. Cavender, D. M. Brennan, W. Koenig, J. W. Jukema, V. Nambi, et al; VISTA-16 Investigators. 2014. Varespladib and cardiovascular events in patients with an acute coronary syndrome: the VISTA-16 randomized clinical trial. *JAMA* 311: 252–262.

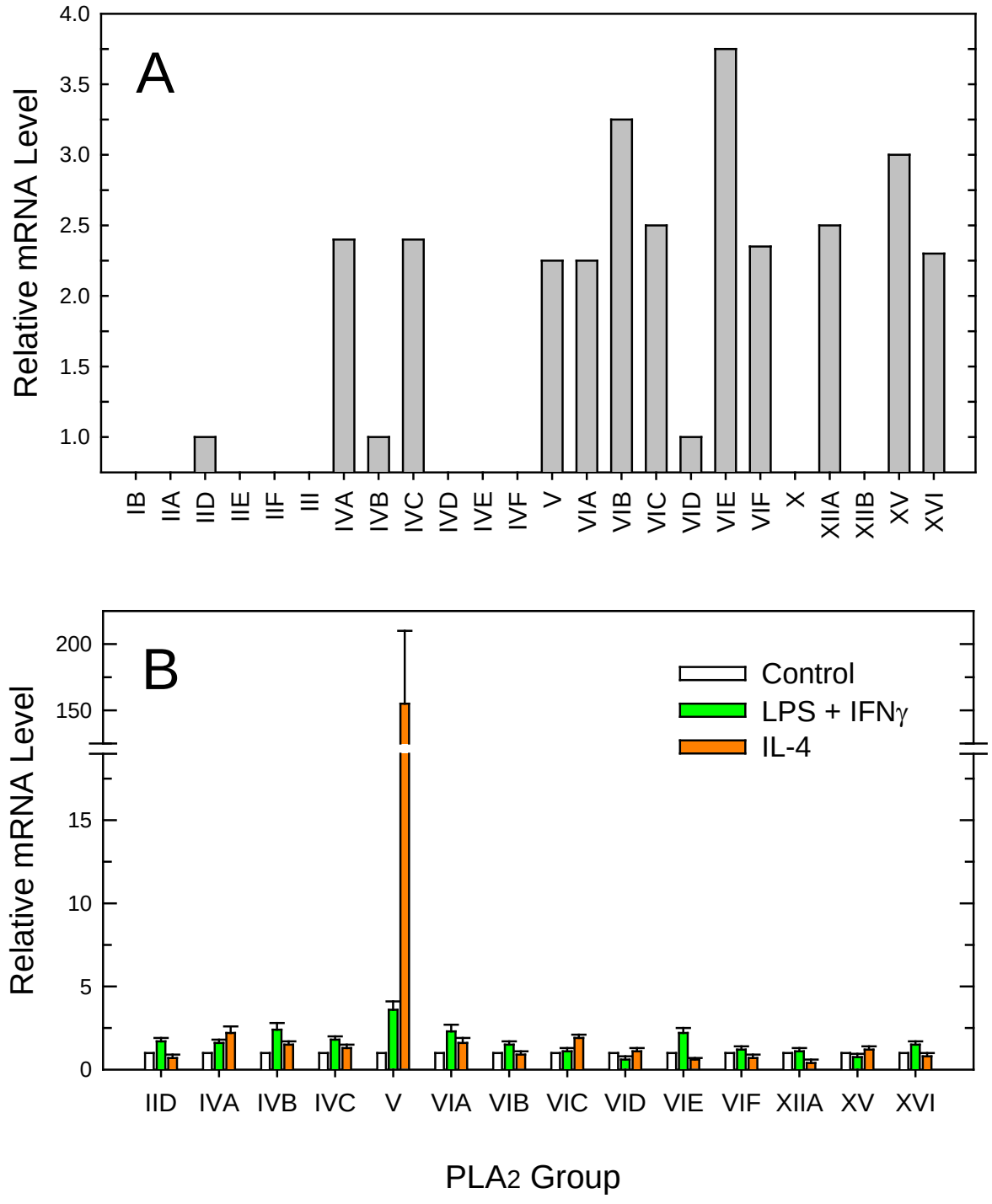

Supplemental Figure 1 – A) Expression of PLA_2 forms in human macrophages, as determined by qPCR. B) Effect of a 24-h treatment with 500 U/ml IFNγ plus 10 ng/ml LPS (green bars) or 1,000 U/ml IL-4 (orange bars) on the expression level of PLA_2 forms, as determined by qPCR. Data are average of three independent experiments with triplicate determinations (mean ± S.E.M.).

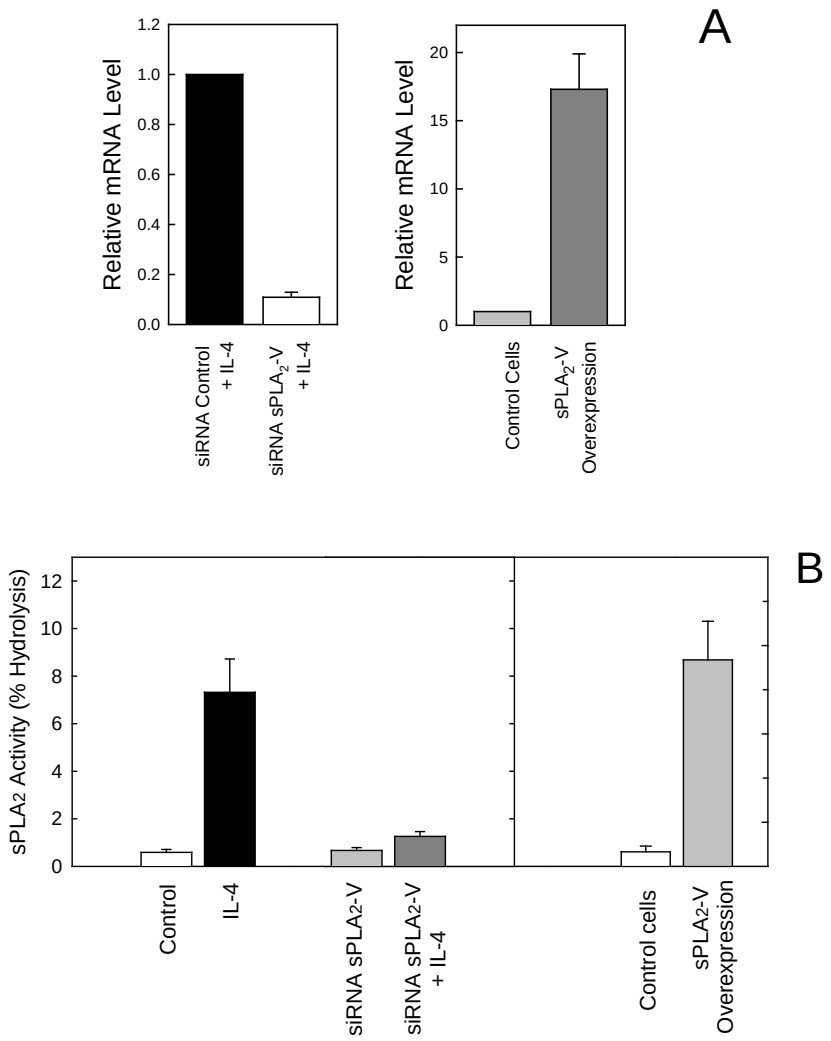

Supplemental Figure 2 – A) qPCR analysis of $sPLA_2$-V levels. Left panel: cells were transfected with control siRNA (closed bar) or siRNA against $sPLA_2$-V (open bar), and after a 24-h treatment with 1,000 U/ml IL-4, the levels of mRNA expression for $sPLA_2$-V were analyzed by qPCR. Right panel: mRNA expression levels for $sPLA_2$-V were analyzed in macrophages overexpressing an empty plasmid (light gray bar) or a plasmid containing human $sPLA_2$-V (dark gray bar). Data are representative of at least three independent experiments. Error bars represent ± SEM. (n=3). B) $sPLA_2$ activity of human macrophage homogenates. Left panel: homogenates were prepared from untreated cells without (open bar) or with (gray bar) siRNA to $sPLA_2$-V, or cells treated with 1,000 U/ml IL-4 without (black bar) or with (dark gray bar) siRNA to $sPLA_2$-V, as indicated. Right panel: homogenates were prepared from cells overexpressing a plasmid containing $sPLA_2$-V (gray bar) or an empty vector (open bar). PLA_2 activity in the homogenates was assayed using a [^{3}H]AA-labeled natural membrane substrate, as detailed in Materials and Methods. Data are shown as means ± SEM of three independent determinations from different homogenate samples.

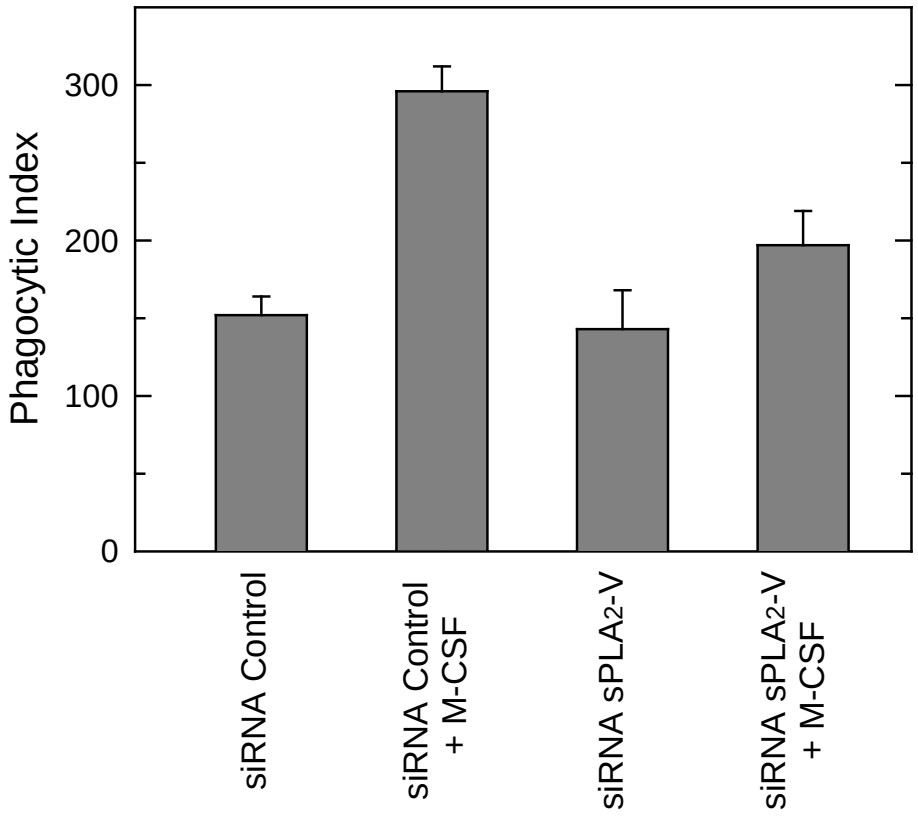

Supplemental Figure 3 – $sPLA_2$-V is involved in the phagocytosis of zymosan by M-CSF-treated macrophages. Human macrophages, either untreated (control) or treated with 50 ng/ml M-CSF for 24 h, and treated with siRNA control or siRNA for $sPLA_2$-V, as indicated, were analyzed for phagocytosis of fluorescent zymosan particles by confocal microscopy, and a phagocytic index was calculated by dividing the number of phagosomes by the total number of cells in a field, which was multiplied by the percentage of phagocytosing cells. Data are shown as means ± SEM of three independent experiments.

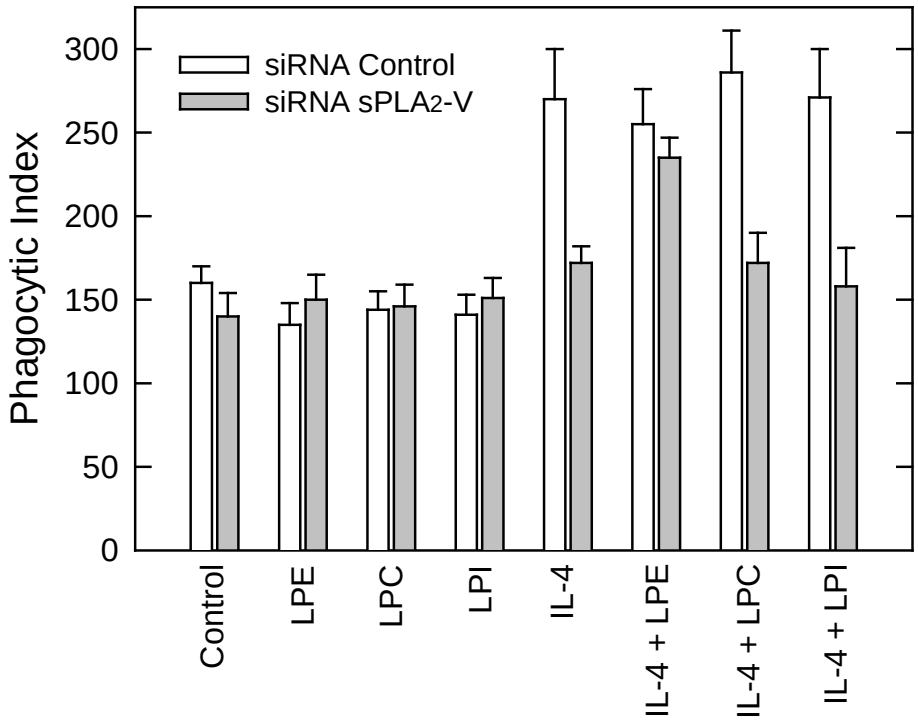

Supplemental Figure 4 – Effect of various lysophospholipids on the phagocytosis of zymosan by IL-4-treated macrophages. Human macrophages, either untreated or treated with 1,000 U/ml IL-4 for 24 h, as indicated, were analyzed for phagocytosis of zymosan particles. The cells were treated with siRNA control or siRNA for $sPLA_2$-V as indicated. Where indicated, LPE, LPC or LPI (5 μM) were added. A phagocytic index was calculated by dividing the number of phagosomes by the total number of cells in a field, which was multiplied by the percentage of phagocytosing cells. The average of three independent experiments with triplicate determinations is shown (mean ± S.E.M.).